Chemical Transformations on Phosphido-Bridged Clusters. Reactions of the μ_3-η^3-Allenyl Complex $Ru_3(CO)_8\{\mu_3$-η^3-$CH_2CC(i\text{-}Pr)\}(\mu\text{-}PPh_2)$. Reversible CO Addition, Adduct Formation with $P(OMe)_3$, Hydrogenation, and Alkyne Insertion

Donato Nucciarone, Nicholas J. Taylor, and Arthur J. Carty*

Guelph-Waterloo Centre for Graduate Work in Chemistry, Waterloo Campus, Department of Chemistry, University of Waterloo, Waterloo, Ontario, Canada N2L 3G1

Received April 8, 1987

Reactions of the allenyl cluster $Ru_3(CO)_8\{\mu_3$-η^3-$CH_2CC(i\text{-}Pr)\}(\mu\text{-}PPh_2)$ (1) with carbon monoxide, trimethyl phosphite, dihydrogen, and alkynes are described. Addition of CO to 1 affords the 50-electron "open" cluster $Ru_3(CO)_9\{\mu_3$-η^3-$CH_2CC(i\text{-}Pr)\}(\mu\text{-}PPh_2)$ (3) via cleavage of the Ru–Ru bond bridged by the phosphido group. Labeling experiments (^{13}CO) indicate regiospecific incorporation of the nucleophile trans to one arm of the phosphido bridge. Trimethyl phosphite reacts similarly giving an open 50-electron cluster 4. Complex 1 activates molecular hydrogen at room temperature and 1 atm leading to conversion of the allenyl group to a μ_3-$\parallel$-acetylene hydride $(\mu\text{-}H)Ru_3(CO)_8\{\mu_3$-$\eta^2$-$CH_3C{\equiv}C(i\text{-}Pr)\}(\mu\text{-}PPh_2)$ (5). Crystals of 5 from *n*-hexane are monoclinic, space group $P2_1/c$, with a = 14.582 (2) Å, b = 11.404 (3) Å, c = 18.496 (3) Å, β = 111.71 (1)°, V = 2857.6 (9) Å^3, and Z = 4. The structure was solved by heavy-atom methods and refined to R and R_w values of 0.030 and 0.034, respectively, using 4170 observed reflections. The molecule consists of an asymmetric triangle of ruthenium atoms with a hydrido bridge across the Ru(1)–Ru(3) edge, a μ-PPh_2 group bridging the Ru(1)–Ru(2) vector, and a multisite bound isopropylmethylacetylene ligand on the top face of the cluster. The conversion of 1 to 5 represents a useful synthetic route to unsymmetrical trinuclear acetylene clusters. In solution 5 exists as interconverting isomers. The reaction of 1 with alkynes results in coupling of the allenyl group and the acetylene to give the clusters $Ru_3(CO)_7\{\mu_3$-η^5-$CH_2CC(i\text{-}Pr)C(R)$-$C(R')\}(\mu\text{-}PPh_2)$ (R = R′ = Ph, 6; R = CH_3, R′ = *i*-Pr, 7; R = *i*-Pr, R′ = CH_3, 8; R = R′ = H, 9) which contain a "wrap-around" five-carbon hydrocarbon chain. Single-crystal X-ray analyses of 6 (crystal data: a = 12.130 (2) Å, b = 16.424 (2) Å, c = 18.766 (3) Å, β = 101.52 (1)°, V = 366.3 (8) Å^3, Z = 4; R = 0.33, R_w = 0.038 on 6363 observed reflections) and 8 (crystal data: a = 9.690 (1) Å, b = 31.287 (5) Å, c = 10.908 (2) Å, β = 106.40 (1)°, V = 3172 (1) Å^3; Z = 4; R = 0.027; R_w = 0.032 on 4407 observed reflections) have revealed that while the hydrocarbyl–Ru_3 frameworks are remarkably similar, the phosphido group is axial to the Ru_3 triangle in 6 and equatorial in 8. The variable-temperature NMR spectra of 7–9 are explicable in terms of a "hidden partner" exchange process involving axial–equatorial phosphido bridge isomerism.

In a preceding paper[1] we reported the synthesis of the allenyl cluster $Ru_3(CO)_8\{\mu_3$-η^3-$CH_2CC(i\text{-}Pr)\}(\mu\text{-}PPh_2)$ (1) via methylene (CH_2) addition to the acetylide $Ru_3(CO)_6$-$(\mu\text{-}CO)_2\{\mu_3$-η^2-$C{\equiv}C(i\text{-}Pr)\}(\mu\text{-}PPh_2)$ (2). Like its isoelectronic 48-electron acetylide counterpart, 2, cluster 1 behaves as if it is coordinatively unsaturated, adding nucleophiles with great facility at ambient temperatures. Lewis base additions to clusters *without* ligand dissociation have been observed recently for several other systems,[2,3] but only in very few cases have the scope and synthetic implications of such reactivity been explored. Here we report a series of reactions of the cluster 1 including reversible CO addition, formation of a phosphite adduct, a novel hydrogenation of the unsaturated ligand, and a series of alkyne insertions leading to hydrocarbon chain extension.

Experimental Section

General experimental procedures have been reported elsewhere.[1] H_2 (Linde), ^{13}CO (Monsanto, 94.8% ^{13}C), $P(OMe)_3$ (Strem Chemical), HC≡CH (Linde), $CH_3C{\equiv}C(i\text{-}Pr)$ (Farchan Acetylenes), PhC≡CPh (Aldrich Chemical Co.), and HC≡CPh (Baker) were used as obtained without further purification. The synthesis of $Ru_3(CO)_8\{\mu_3$-η^3-$CH_2C_2(i\text{-}Pr)\}(\mu\text{-}PPh_2)$ (1) has been described in the first paper in this series.[1]

Preparation of $Ru_3(CO)_9\{\mu_3$-η^3-$CH_2C_2(i\text{-}Pr)\}(\mu\text{-}PPh_2)$ (3). Bubbling CO through heptane solutions of 1 resulted in a rapid color change from maroon to yellow indicating the formation of 3. The reaction progress was monitored by IR spectroscopy, and only one product was observed. Attempts to isolate 3 as a solid were unsuccessful but yields are believed to be quantitative on the basis of NMR and IR results and the lack of decomposition during the course of the reaction.

(1) Nucciarone, D.; MacLaughlin, S. A.; Taylor, N. J.; Carty, A. J. *Organometallics*, first of three papers in this issue.

(2) For recent reviews see: (a) Johnson, B. F. G., Ed. *Transition Metal Clusters*; Wiley: New York, 1980. (b) Johnson, B. F. G.; Lewis, J. *Adv. Inorg. Chem. Radiochem.* **1981**, *24*, 225. (c) Adams, R. D.; Horvath, I. T. *Prog. Inorg. Chem.* **1985**, *33*, 127. (d) Vahrenkamp, H. *Angew. Chem., Int. Ed. Engl.* **1978**, *17*, 379. (e) Vahrenkamp, H. *Adv. Organomet. Chem.* **1983**, *22*, 169.

(3) See for example: (a) Huttner, G.; Schneider, J.; Muller, H. D.; Mohr, G.; v. Seyerl, J.; Wohlfahrt, L. *Angew. Chem., Int. Ed. Engl.* **1979**, *18*, 76. (b) Langenbach, H. J.; Vahrenkamp, H. *Chem. Ber.* **1979**, *112*, 3390. (c) Sivak, A. J.; Muetterties, E. L. *J. Am. Chem. Soc.* **1979**, *101*, 4878. (d) Carty, A. J.; MacLaughlin, S. A.; Taylor, N. J. *J. Organomet. Chem.* **1981**, *204*, C27. (e) Richter, F.; Vahrenkamp, H. *Organometallics* **1982**, *1*, 756. (f) Vahrenkamp, H.; Wolters, D. *Organometallics* **1982**, *1*, 874. (g) Lesch, D. A.; Rauchfuss, T. B. *Organometallics* **1982**, *1*, 499. (h) Johnson, B. F. G.; Lewis, J.; Nicholls, J. N.; Puga, J.; Raithby, P. R.; Rosales, M. J.; McPartlin, M.; Clegg, W. *J. Chem. Soc., Dalton Trans.* **1983**, 277. (i) Cowie, A. G.; Johnson, B. F. G.; Nicholls, J. N.; Raithby, P. R.; Rosales, M. J. *J. Chem. Soc., Dalton Trans.* **1983**, 2311. (j) Schneider, J.; Hüttner, G. *Chem. Ber.* **1983**, *116*, 917. (k) Jones, R. A.; Wright, T. C.; Atwood, J. L.; Hunter, W. E. *Organometallics* **1983**, *2*, 470. (l) MacLaughlin, S. A.; Taylor, N. J.; Carty, A. J. *Organometallics* **1983**, *2*, 1194. (m) Dawoodi, Z.; Mays, M. J. *J. Chem. Soc., Dalton Trans.* **1984**, 1931. (n) Richter, F.; Muller, M.; Gartner, N.; Vahrenkamp, H. *Chem. Ber.* **1984**, *117*, 2438. (o) Morrison, E. D.; Geoffroy, G. L.; Rheingold, A. L.; Fultz, W. C. *Organometallics* **1985**, *4*, 1413. (p) Adams, R. D.; Wang, S. *Organometallics* **1985**, *4*, 1902. (q) Farrugia, L. J.; Green, M.; Hankey, D. R.; Murray, M.; Orpen, A. G.; Stone, F. G. A. *J. Chem. Soc., Dalton Trans.* **1985**, 177.

0276-7333/88/2307-0127$01.50/0

Table I. Summary of Crystal Data, Intensity Collection, Reduction, and Refinement for Clusters 5, 6, and 8

	5	6	8
mol formula	$(\mu\text{-H})Ru_3(CO)_8\{\mu_3\text{-}\eta^2\text{-}CH_3C{\equiv}C\text{-}(i\text{-Pr})\}(\mu\text{-}PPh_2)$	$Ru_3(CO)_7\{\mu_3\text{-}\eta^5\text{-}CH_2{=}C{=}C\text{-}(i\text{-Pr})C(Ph)C(Ph)\}(\mu\text{-}PPh_2)$	$Ru_3(CO)_7\{\mu_3\text{-}\eta^5\text{-}CH_2{=}C{=}C\text{-}(i\text{-Pr})C(i\text{-Pr})C(Me)\}(\mu\text{-}PPh_2)$
empirical formula	$Ru_3PO_8C_{26}H_{21}$	$Ru_3PO_7C_{39}H_{29}$	$Ru_3PO_7C_{31}H_{29}$
mol wt	795.64	943.85	847.76
cryst system	monoclinic	monoclinic	monoclinic
space group	$P2_1/n$	$P2_1$	$P2_1/n$
a, (Å)	14.582 (2)	12.130 (2)	9.690 (1)
b, (Å)	11.404 (3)	16.424 (2)	31.287 (5)
c, (Å)	18.496 (3)	18.766 (3)	10.908 (2)
β, deg	111.71 (1)	101.52 (1)	106.40 (1)
V, Å^3	2857.6 (9)	3663.3 (8)	3172 (1)
d_{calcd}, g·cm^{-3}	1.849	1.711	1.775
$d_{measd}(CCl_4/C_2H_2Br_4)$, g·cm^{-3}	1.85	1.72	1.77
Z	4	4	4
$F(000)$, electrons	1552	1864	1672
cryst size, mm	0.27 × 0.30 × 0.31	0.27 × 0.18 × 0.29	0.25 × 0.28 × 0.31
radiatn λ, Å	0.71069	0.71069	0.71069
μ(Mo Kα), cm^{-1}	16.30	12.86	14.72
scan mode	$\theta/2\theta$	$\theta/2\theta$	$\theta/2\theta$
scan speed, deg·min^{-1}	2.93–29.30	2.93–29.30	1.50–29.30
2θ range, deg	3.2–50.0	3.2–50.0	3.2–50.0
std reflctns	008; 806	080; 500	0,20,0; 400
change in std, %	±2	±2	±2
no. of reflctns measd	5065	6737	5592
no. of reflctns obsd	4170	6363	4407
transmissn factors	0.54–0.72	0.63–0.77	0.59–0.76
R^a	0.030	0.033[c]	0.027
R_w[b]	0.034	0.038	0.032
weighting scheme	$w^{-1} = 1.98 - 0.0135\|F_o\| + 0.0017\|F_o\|^2$	$w^{-1} = 2.22 - 0.0152\|F_o\| + 0.00028\|F_o\|^2$	$w^{-1} = 1.65 - 0.0211\|F_o\| + 0.00023\|F_o\|^2$
final diff map electron density, e·Å^{-3}	0.95	0.9	0.5

[a] $R = \sum(||F_o| - |F_c||)/\sum|F_o|$. [b] $R_w = [\sum_w(|F_o| - |F_c|)^2/\sum_w(|F_o|)^2]^{1/2}$. [c] $R = 0.03392$ for xyz and 0.03311 for $x\bar{y}z$.

Samples for ^{31}P and ^{13}C NMR studies were prepared by bubbling a slow stream of CO through a $CDCl_3$ solution of **1** (50 mg, 0.063 mmol) in a 10-mm NMR tube held in a dry ice/acetone bath (ca. 30 s for complete conversion as noted by color changes). This sample was then capped and transferred to the NMR spectrometer for analysis. Samples of **3** prepared specifically for ^{13}CO-labeling studies were prepared in a similar fashion. IR (C_6H_{12}): ν(CO) 2083 s, 2059 vs, 2034 vs, 2017 vs, 2011 vs, 1999 s, 1987 m, 1975 s cm^{-1}. $^{31}P\{^1H\}$ NMR (chloroform-*d*, −60 °C): δ −23.1. ^1H NMR (chloroform-*d*, 30 °C): δ 1.15 (d, J = 6 Hz, CH_3, 3 H), 1.47 (d, J = 6 Hz, CH_3, 3 H), 3.08 (d, J = 3 Hz, CH_2, 1 H), 3.22 (m, J = 6 Hz, $CH(CH_3)_2$, 1 H), 3.33 (d, J = 3 Hz, CH_2, 1 H), 6.8–7.7 (m, phenyl ring hydrogens). ^{13}C NMR (chloroform-*d*, −60 °C): δ 24.8 (q, J_{CH} = 123 Hz, $CHCH_3$), 27.7 (q, J_{CH} = 122 Hz, $CHCH_3$), 32.5 (t, J_{CH} = 160 Hz, C=C=CH_2), 47.9 (d, J_{CH} = 133 Hz, $CHCH_3$), 127–134 (phenyl ring carbons), 136.4 (d, J_{PC} = 28 Hz, ipso-C), 141.7 (d, J_{PC} = 19 Hz, ipso-C), 158.0 (s, C=C=CH_2), 190.8 (s, 1 CO), 191.1 (d, J_{PC} = 69 Hz, 1 CO), 193.9 (d, J_{PC} = 90 Hz, 1 CO), 194.0 (d, J_{PC} = 10 Hz, 1 CO), 194.9 (s, 1 CO), 195.4 (s, 1 CO), 198.2 (d, J_{PC} = 7 Hz, 1 CO), 198.9 (s, 1 CO), 199.1 (s, 1 CO), 213.6 (s, C=C=CH_2).

Preparation of $Ru_3(CO)_8(P(OMe)_3)\{\mu_3\text{-}\eta^3\text{-}CH_2C_2(i\text{-Pr})\}(\mu\text{-}PPh_2)$ (4). To a 10-mm NMR tube containing **1** (100 mg, 0.126 mmol) in CD_2Cl_2 (1 mL) at dry ice temperature was added 1 equiv of $P(OMe)_3$ (15 μL diluted with 2 mL of CD_2Cl_2). An immediate color change from maroon to yellow was noted similar to that observed when CO was bubbled through solutions of **1**. This sample was then placed in the NMR spectrometer, precooled to −70 °C, for analysis. IR (C_6H_{12}): ν(CO) 2064 s, 2033 s, 2027 m, sh, 2013 s, 1999 m, 1994 m, 1980 m, 1961 m cm^{-1}. $^{31}P\{^1H\}$ NMR (methylene-d_2 chloride, −70 °C): δ −7.2 (d, J_{PP} = 314 Hz, PPh_2), 135.9 (d, J_{PP} = 314 Hz, $P(OMe)_3$). ^1H NMR (methylene-d_2 chloride, −60 °C): 1.28 (d, J = 6 Hz, $CHCH_3$, 3 H), 1.58 (d, J = 6 Hz, $CHCH_3$, 3 H), 3.31 (s, CH_2, 1 H), 3.46 (s, CH_2, 1 H), 3.77 (d, $^3J_{PH}$ = 20 Hz, $P(OCH_3)_3$, 9 H), 6.93–7.65 (phenyl ring hydrogens).

Preparation of $(\mu\text{-H})Ru_3(CO)_8(\mu_3\text{-}\eta^2\text{-}CH_3C_2(i\text{-Pr}))(\mu\text{-}PPh_2)$ (5). A solution containing **1** (200 mg, 0.252 mmol) in hexane (40 mL) was cooled in an ice/water bath. Hydrogen gas was bubbled through the solution for 3 h. The solution was concentrated and chromatographed on Florisil. Eluting with hexane separated three products. The first and third bands, which were yellow and green in color, respectively, were obtained in very small quantities and were not characterized. The major product was the second, orange, band identified as **5**. Concentration and cooling of hexane solutions of this fraction produced, upon addition of a seed crystal, good yields of red crystals of **5** (174 mg, 86%). Some decomposition on the column during chromatography was noted. Solutions of **5** slowly decompose on standing thus actual yields are probably higher than the isolated yields reported. Anal. Calcd for $C_{26}H_{21}O_8PRu_3$: C, 39.25; H, 2.66; P, 3.89; Found: C, 39.33; H, 2.60; P, 4.01. IR (C_6H_{12}): ν(CO) 2074 m, 2036 s, 2022 s, 2012 s, 1981 s, 1964 m, 1864 m cm^{-1}. ^1H NMR (chloroform-*d*, −40 °C): isomer A, δ −16.28 (d, J_{PH} = 15 Hz, μ-H), −0.43 (d, J = 6 Hz, $CHCH_3$), 2.08 (sept, J = 6 Hz, $CH(CH_3)_2$), 7.24–7.99 (phenyl ring hydrogens); isomer B, δ −14.87 (d, J_{PH} = 18 Hz, μ-H), 0.74 (d, J = 6 Hz, $CHCH_3$), 1.26 (d, J = 6 Hz, $CHCH_3$), 2.95 (sept, J = 6 Hz, $CH(CH_3)_2$, 3.03 (s, CCH_3), 7.24–7.99 (phenyl ring hydrogens). ^1H NMR (toluene-d_8, −20 °C): isomer A, −15.96 (d, J_{PH} = 15 Hz, μ-H), −0.44 (d, J = 7 Hz, $CHCH_3$), 0.94 (d, J = 6 Hz, $CHCH_3$), 1.70 (s, CCH_3), 1.98 (m, J = 7 Hz, $CH(CH_3)_2$), 6.82–7.93 (m, phenyl ring hydrogens); isomer B, −14.52 (d, J_{PH} = 18 Hz, μ-H), 0.86 (d, J = 6 Hz, $CHCH_3$), 1.27 (d, J = 6 Hz, $CHCH_3$), 2.75 (sept, J = 6 Hz, $CH(CH_3)_2$), 2.85 (s, CCH_3), 6.82–7.93 (m, phenyl ring hydrogens). $^{31}P\{^1H\}$ NMR (chloroform-*d*, −40 °C): isomer A, δ 242.2 (s); isomer B, δ 265.3 (s). $^{31}P\{^1H\}$ NMR (toluene-d_8, −20 °C): isomer A, δ 242.7 (s); isomer B, δ 265.0 (s).

Preparation of $Ru_3(CO)_7(\mu_3\text{-}\eta^5\text{-}CH_2C_2(i\text{-Pr})C(R)C(R'))(\mu\text{-}PPh_2)$. R = R′ = Ph, 6. A toluene solution (15 mL) containing **1** (200 mg, 0.252 mmol) and diphenylacetylene (68 mg, 0.378 mmol) was heated for 4 days at 55 °C before being taken to dryness. Chromatography by preparative TLC gave only two bands which were eluted with hexane. The first band was starting material (64 mg, 32% recovery) followed by a pinkish red band of **6**. Crystallization gave 129 mg of **6** (82% yield based on reacted starting material). Anal. Calcd for $C_{39}H_{29}O_7PRu_3$: C, 49.63; H, 3.40; P, 3.28. Found: C, 49.41; H, 3.17; P, 3.73. IR (C_6H_{12}): ν(CO) 2064 s, 2023 s, 2006 s, 2001 w, sh, 1966 m, 1960 w, 1954 m cm^{-1}.

$^{31}P\{^1H\}$ NMR (chloroform-*d*, 30 °C): δ 249.4 (s). ^1H NMR (chloroform-*d*, 30 °C): δ 0.40 (s, br, 3 H), 1.12 (s, br, 4 H), 3.25 (AB doublet, *J* = 3 Hz, CH_2, 1 H), 3.38 (AB doublet, *J* = 3 Hz, CH_2, 1 H), 6.8–7.9 (m, phenyl ring hydrogens).

R = CH_3, R′ = *i*-Pr, 7; R = *i*-Pr, R′ = CH_3, 8. The reaction was carried out as for **6** above replacing diphenylacetylene with methylisopropylacetylene and modifying conditions such that the reaction was allowed to proceed for 2 days at 65–70 °C. Chromatography by preparative TLC gave three bands: an orange, first band containing a mixture of **7** and **8** (combined yield of 156 mg, 73%, based on reacted starting material) followed by a second band of starting material (30 mg, 15% recovery) and a third, purple band obtained in minute quantities and not characterized. Attempts to physically separate isomeric **7** and **8** in substantial quantities were not successful although fractional crystallization could selectively enhance the presence of one form over the other and a single crystal of **8** was picked for X-ray analysis. Anal. Calcd for $C_{31}H_{29}O_7PRu_3$: C, 43.92; H, 3.45; P, 3.65. Found: C, 43.97; H, 3.73; P, 3.34. IR (C_6H_{12}): ν(CO) 2055 m, 2019 s, 2011 s, 1995 m, 1980 w, 1961 m cm^{-1} $^{31}P\{^1H\}$ NMR (methylene-d_2, chloride, 27 °C): for **8**, δ 220.6 (s, $\Delta\nu_{1/2}$ = 51 Hz); for **7** δ 229.2 (s, $\Delta\nu_{1/2}$ = 130 Hz). ^1H NMR for compound **8** (methylene-d_2 chloride, −70 °C): δ 0.49 (d, *J* = 7 Hz, $CHCH_3$), 1.38 (d, *J* = 7 Hz, $CHCH_3$), 1.53 (sept, *J* = 7 Hz, $CHCH_3$), 1.58 (d, *J* = 7 Hz, $CHCH_3$), 1.66 (d, *J* = 7 Hz, $CHCH_3$), 3.08 (s, $C{=}CCH_3$), 3.10 (sept, *J* = 7 Hz, $CHCH_3$), 3.80 (s, CH_2), 4.40 (s, CH_2), 7.22–7.69 (m, phenyl ring hydrogens). ^1H NMR for compound **7** (methylene-d_2 chloride, −30 °C): δ 0.50 (d, *J* = 7 Hz, $CHCH_3$), 1.23 (d, *J* = 6 Hz, $CHCH_3$), 1.34 (d, *J* = 6 Hz, $CHCH_3$), 1.35 (d, *J* = 7 Hz, $CHCH_3$), 1.58 (br, $CHCH_3$), 2.61 (s, $C{=}CCH_3$), 3.57 (br, $CHCH_3$), 3.92 (br, CH_2), 4.50 (br, CH_2), 7.27–7.72 (m, phenyl ring hydrogens).

R = R′ = H, 9. A toluene solution (25 mL) of **1** (200 mg, 0.252 mmol) was held in a two-necked, 250-mL, round-bottom flask. One neck provided an inlet port for acetylene gas while the other neck was connected to an oil bubbler. The flask was purged for ca. $^1/_2$ h with acetylene. Gas flow was stopped and the flask immersed in an oil bath preheated at 65 °C and left stirring under a static atmosphere of acetylene for 2 h whereupon the heat was turned off. The flask was allowed to cool to room temperature, while still immersed, and left stirring for an additional total of 10 h. Column chromatography on Florisil eluting with heptane gave an orange band as the major product. Considerable decomposition was noted. Subsequent crystallization of the orange band from hexane gave 32 mg (16%) of **9**. Anal. Calcd for $C_{27}H_{21}O_7PRu_3$: C, 40.97; H, 2.97. Found: C, 40.78; H, 2.91. IR (C_6H_{12}): ν(CO) 2062 m, 2024 m, 2017 s, 2002 m, 1985 w, 1967 m cm^{-1}. $^{31}P\{^1H\}$ NMR (benzene-d_6, 30 °C): δ 222.2 (s). ^1H NMR (benzene-d_6, 30 °C): δ 0.17 (d, *J* = 6 Hz, CH_3, 3 H), 1.07 (s, $CH(CH_3)_2$, 4 H), 4.14 (d, *J* = 2 Hz, CH_2, 1 H), 4.30 (d, *J* = 2 Hz, CH_2, 1 H), 5.64 (d, *J* = 5 Hz, C(*H*)C(H)Ru, 1 H), 6.9–7.7 (m, phenyl ring hydrogens), 8.64 (d, *J* = 5 Hz, C(H)C(*H*)Ru, 1 H).

X-ray Structure Analyses of 5, 6, and 8. Crystals of the μ-hydrido, μ_3-acetylene cluster **5**, precipitated from *n*-hexane, were red prisms. The acetylene insertion products **6** (R = R′ = Ph) and **8** (R = *i*-Pr, R′ = Me) (from *n*-hexane) were pinkish red and orange, respectively.

Crystal data for all three compounds are listed in Table I. Instrumental parameters for intensity data collection and information on the subsequent treatment of diffraction data are also listed in Table I. Procedures were similar for all three compounds, and only a brief description is given here for **5**.

A crystal of dimensions 0.27 × 0.30 × 0.31 mm was cemented onto a brass pin with epoxy resin, attached to a goniometer head and mounted on a Syntex $P2_1$ diffractometer for preliminary unit cell measurements. Rotation photographs and initial counter data indicated a monoclinic unit cell. Using the Syntex autoindexing and cell refinement routines, least-squares refinement of the settings for 15 reflections afforded the unit cell parameters listed in Table I. Intensity data were collected on the same crystal using Mo Kα (λ = 0.710 69 Å) radiation and θ–2θ scans as described in Table I. During data collection two standard reflections (008 and 806) monitored every 100 measurements decreased in intensity by ±2%. Appropriate scaling was applied to reduce the intensities to a common level. Lorentz and polarization corrections were made and the intensities converted to structure factors in the normal way. The structure was solved by heavy-atom methods using the full set of 4170 observed ($I \geq 3\sigma(I)$) unique reflections and refined by full-matrix least-squares methods, first with isotropic and subsequently with anisotropic coefficients. Hydrogen atom positions were readily located from a difference Fourier map for **5**. In subsequent refinements hydrogen atom positions and

Table II. A Compilation of Important Bond Lengths (Å) and Angles (deg) for (μ-H)$Ru_3(CO)_8\{\mu_3$-η^2-$CH_3C{=}C(i$-Pr)$\}(\mu$-$PPh_2)$ (5)

(a) Bond Lengths

Ru(1)–Ru(2)	2.7538 (5)	Ru(1)–Ru(3)	2.8135 (4)
Ru(2)–Ru(3)	2.8351 (5)	Ru(1)–P	2.262 (1)
Ru(2)–P	2.420 (1)	Ru(1)–C(1)	1.881 (5)
Ru(1)–C(2)	1.888 (6)	Ru(2)–C(3)	1.908 (6)
Ru(2)–C(4)	1.947 (6)	Ru(2)–C(5)	1.926 (5)
Ru(3)–C(6)	1.923 (6)	Ru(3)–C(7)	1.908 (5)
Ru(3)–C(8)	1.947 (6)	Ru(1)–C(10)	2.144 (5)
Ru(2)–C(10)	2.243 (5)	Ru(1)–C(11)	2.317 (4)
Ru(3)–C(11)	2.168 (4)	Ru(1)–H(1)	1.67 (6)
Ru(3)–H(1)	1.76 (6)	P–C(15)	1.825 (4)
P–C(21)	1.819 (5)	C(1)O(1)	1.131 (6)
C(2)–O(2)	1.126 (8)	C(3)–O(3)	1.141 (8)
C(4)–O(4)	1.121 (8)	C(5)–O(5)	1.127 (7)
C(6)–O(6)	1.125 (8)	C(7)–O(7)	1.129 (7)
C(8)–O(8)	1.127 (7)	C(9)–C(10)	1.525 (8)
C(10)–C(11)	1.311 (6)	C(11)–C(12)	1.521 (6)
C(12)–C(13)	1.515 (9)	C(12)–C(14)	1.500 (12)

(b) Bond Angles

Ru(2)–Ru(1)–Ru(3)	61.22 (1)	Ru(2)–Ru(1)–P	56.67 (2)
Ru(2)–Ru(1)–C(1)	107.8 (1)	Ru(2)–Ru(1)–C(2)	159.5 (1)
Ru(2)–Ru(1)–C(10)	52.7 (1)	Ru(2)–Ru(1)–C(11)	71.7 (1)
Ru(2)–Ru(1)–H(1)	83 (2)	Ru(3)–Ru(1)–P	91.95 (2)
Ru(3)–Ru(1)–C(1)	158.8 (1)	Ru(3)–Ru(1)–C(2)	106.4 (1)
Ru(3)–Ru(1)–C(10)	69.0 (1)	Ru(3)–Ru(1)–C(11)	48.8 (1)
Ru(3)–Ru(1)–H(1)	36 (2)	P–Ru(1)–C(1)	96.2 (1)
P–Ru(1)–C(2)	110.9 (1)	P–Ru(1)–C(10)	107.3 (1)
P–Ru(1)–C(11)	126.8 (1)	P–Ru(1)–H(1)	81 (2)
C(1)–Ru(1)–C(2)	88.9 (2)	C(1)–Ru(1)–C(10)	89.9 (2)
C(1)–Ru(1)–C(11)	111.9 (1)	C(1)–Ru(1)–H(1)	165 (2)
C(2)–Ru(1)–C(10)	141.7 (2)	C(2)–Ru(1)–C(11)	113.8 (1)
C(2)–Ru(1)–H(1)	79 (2)	C(10)–Ru(1)–C(11)	33.9 (1)
C(10)–Ru(1)–H(1)	105 (2)	C(11)–Ru(1)–H(1)	81 (2)
Ru(1)–Ru(2)–Ru(3)	60.43 (1)	Ru(1)–Ru(2)–P	51.35 (2)
Ru(1)–Ru(2)–C(3)	120.6 (1)	Ru(1)–Ru(2)–C(4)	113.8 (1)
Ru(1)–Ru(2)–C(5)	130.7 (1)	Ru(1)–Ru(2)–C(10)	49.5 (1)
Ru(3)–Ru(2)–P	88.21 (2)	Ru(3)–Ru(2)–C(3)	83.5 (1)
Ru(3)–Ru(2)–C(4)	169.7 (1)	Ru(3)–Ru(2)–C(5)	92.5 (1)
Ru(3)–Ru(2)–C(10)	67.5 (1)	P–Ru(2)–C(3)	170.9 (1)
P–Ru(2)–C(4)	94.2 (1)	P–Ru(2)–C(5)	91.1 (1)
P–Ru(2)–C(10)	99.1 (1)	C(3)–Ru(2)–C(4)	93.4 (2)
C(3)–Ru(2)–C(5)	92.8 (2)	C(3)–Ru(2)–C(11)	74.4 (2)
C(4)–Ru(2)–C(5)	97.4 (2)	C(4)–Ru(2)–C(11)	102.3 (2)
C(5)–Ru(2)–C(11)	157.0 (2)	Ru(1)–Ru(3)–Ru(2)	58.4 (0)
Ru(1)–Ru(3)–C(6)	143.5 (1)	Ru(1)–Ru(3)–C(7)	106.5 (1)
Ru(1)–Ru(3)–C(8)	113.9 (1)	Ru(1)Ru(3)–C(11)	53.5 (1)
Ru(1)–Ru(3)–H(1)	34 (2)	Ru(2)–Ru(3)–C(6)	98.2 (1)
Ru(2)–Ru(3)–C(7)	164.8 (1)	Ru(2)–Ru(3)–C(8)	92.6 (1)
Ru(2)–Ru(3)–C(11)	72.1 (1)	Ru(2)–Ru(3)–H(1)	79 (2)
C(6)–Ru(3)–C(7)	94.5 (2)	C(6)–Ru(3)–C(8)	93.0 (2)
C(6)–Ru(3)–C(11)	94.6 (2)	C(6)–Ru(3)–H(1)	177 (2)
C(7)–Ru(3)–C(8)	95.0 (2)	C(7)–Ru(3)–C(11)	98.7 (1)
C(7)–Ru(3)–H(1)	88 (2)	C(8)–Ru(3)–C(11)	163.7 (1)
C(8)–Ru(3)H(1)	88 (2)	C(11)–Ru(3)–H(1)	84 (2)
Ru(1)–P–Ru(2)	71.97 (2)	Ru(1)–P–C(15)	119.5 (1)
Ru(1)–P–C(21)	123.0 (1)	Ru(2)–P–C(15)	121.8 (1)
Ru(2)–P–C(21)	117.4 (1)	C(15)–P–C(21)	102.5 (2)
Ru(1)–C(1)–O(1)	179.0 (2)	Ru(1)–C(2)–O(2)	178.6 (2)
Ru(2)–C(3)–O(3)	175.3 (2)	Ru(2)–C(4)–O(4)	173.2 (2)
Ru(2)–C(5)–O(5)	175.4 (2)	Ru(3)–C(6)–O(6)	177.5 (2)
Ru(3)–C(7)–O(7)	176.8 (2)	Ru(3)–C(8)–O(8)	178.6 (2)
Ru(1)–C(10)–Ru(2)	77.7 (1)	Ru(1)–C(10)–C(9)	127.8 (2)
Ru(1)–C(10)–C(11)	80.3 (1)	Ru(2)–C(10)–C(9)	118.7 (2)
Ru(2)–C(10)–C(11)	112.0 (1)	C(9)–C(10)–C(11)	125.6 (3)
Ru(1)–C(11)–Ru(3)	77.6 (1)	Ru(1)–C(11)–C(10)	65.8 (2)
Ru(1)–C(11)–C(12)	128.6 (1)	Ru(3)–C(11)–C(10)	108.2 (2)
Ru(3)–C(11)–C(12)	126.0 (1)	C(10)–C(11)–C(12)	125.2 (2)
C(11)–C(12)–C(13)	115.7 (3)	C(11)–C(12)–C(14)	109.7 (4)
C(13)–C(12)–C(14)	110.0 (5)		

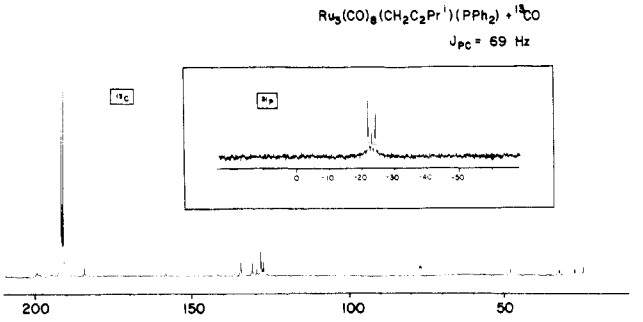

Figure 1. The $^{13}C\{^1H\}$ and (inset) $^{31}P\{^1H\}$ NMR spectra of $Ru_3(CO)_8(^{13}CO)\{\mu_3\text{-}\eta^2\text{-}CH_2CC(i\text{-}Pr)\}(\mu\text{-}PPh_2)$ formed by addition of ^{13}CO at −78 °C to 1.

isotropic thermal parameters were varied. Final R and R_w values were 0.030 and 0.034, respectively. A final difference map was featureless, with a maximum residual electron density of 0.5 eÅ^{-3} in the region of the ruthenium atoms. Atomic scattering factors for heavy atoms were taken from ref 4 and for hydrogen atoms from the compilation of Stewart et al.[5] Anomalous dispersion corrections for the ruthenium atoms were incorporated.[4] Computer programs used have been described elsewhere.[6]

Atomic coordinates for **5**, **6**, and **8** are listed in supplementary Tables S1–S3. A compilation of relevant bond distances and angles (Tables II–IV) is included for each of the three structures. Anisotropic thermal parameters (Tables S4–S6), remaining bond lengths and angles (Tables S7–S9), and structure factors (Tables S10–S12) have been deposited as supplementary material.

Results and Discussion

The allenyl cluster **1** reacts rapidly with carbon monoxide giving bright yellow solutions. Isolation of the product **3** was complicated by its tendency to revert to **1** by loss of CO, and indeed pure crystalline **3** was not isolated. The complex was however readily characterized by spectroscopic methods. Addition of 95% ^{13}CO to cooled solutions of **1** followed by $^{13}C\{^1H\}$ and $^{31}P\{^1H\}$ NMR analyses gave the results depicted in Figure 1. In the ^{13}C NMR spectrum a sharp doublet with a peak separation of 69 Hz is apparent in the terminal CO region. The appearance of a similar doublet in the ^{31}P spectrum with an identical $J_{P\text{-}C}$ of 69 Hz indicates that a single ^{13}CO has added to **1** in a position trans to the phosphido bridge phosphorus atom. At 196 K carbonyl scrambling is slow in comparison to ^{13}CO incorporation into the unique site. The high-field ^{31}P shift (δ −23.1) contrasts sharply with the low-field singlet resonance in **1** (+269.4 ppm) where the μ-PPh_2 group bridges a pair of strongly interacting metals and is consistent with an "open" Ru_3 framework with the phosphido group across the open edge. For comparison, $\delta(^{31}P)$ in the open, 50-electron acetylide cluster $Ru_3(CO)_9\{\mu_3\text{-}\eta^2\text{-}CC(i\text{-}Pr)\}(\mu\text{-}PPh_2)$ is −73 ppm.[1]

Further information on the structure of this new cluster is obtained from the ^{13}C NMR resonance of the isopropyl-substituted, σ-bonded, allenyl carbon atom. The observation of a *singlet* at 213.6 ppm for this carbon atom indicates that this carbon remains bound to the same ruthenium atom as in **1**. The IR spectrum confirms that all nine CO's are terminal. This combined information per-

(4) *International Tables for X-ray Crystallography*; Kynoch: Birmingham, England, 1974; Vol. IV.
(5) Stewart, R. F.; Davidson, E. R.; Simpson, W. T. *J. Chem. Phys.* **1965**, *42*, 3175.
(6) Carty, A. J.; Mott, G. N.; Taylor, N. J.; Yule, J. E. *J. Am. Chem. Soc.* **1978**, *100*, 3051.

Table III. A Compilation of Important Bond Lengths (Å) and Angles (deg) for Molecule A of $Ru_3(CO)_7\{\mu_3\text{-}\eta^5\text{-}CH_2CC(i\text{-}Pr)C(Ph)C(Ph)\}(\mu\text{-}PPh_2)$ (6)

(a) Bond Lengths

Ru(1)–Ru(2)	2.772 (1)	Ru(1)–Ru(3)	2.928 (1)
Ru(2)–Ru(3)	2.833 (1)	Ru(1)–P	2.256 (2)
Ru(3)–P	2.330 (2)	Ru(1)–C(1)	1.887 (9)
Ru(1)–C(2)	1.856 (10)	Ru(2)–C(3)	1.938 (11)
Ru(2)–C(4)	1.960 (11)	Ru(2)–C(5)	1.879 (11)
Ru(3)–C(6)	1.898 (9)	Ru(3)–C(7)	1.883 (10)
Ru(1)–C(8)	2.251 (9)	Ru(1)–C(9)	2.391 (8)
Ru(2)–C(9)	2.051 (8)	Ru(3)–C(10)	2.279 (8)
Ru(3)–C(11)	2.264 (8)	Ru(2)–C(12)	2.127 (8)
Ru(3)–C(12)	2.211 (8)	P–C(28)	1.824 (9)
P–C(34)	1.815 (10)	C(1)–C(1)	1.135 (12)
C(2)–O(2)	1.157 (12)	C(3)–O(3)	1.143 (14)
C(4)–O(4)	1.143 (14)	C(5)–O(5)	1.154 (15)
C(6)–O(6)	1.134 (11)	C(7)–O(7)	1.143 (12)
C(8)–C(9)	1.425 (13)	C(9)–C(10)	1.488 (12)
C(10)–C(11)	1.438 (12)	C(10)–C(13)	1.543 (12)
C(11)–C(12)	1.414 (12)	C(11)–C(16)	1.518 (12)
C(12)–C(22)	1.505 (13)	C(13)–C(14)	1.561 (14)
C(13)–C(15)	1.539 (14)		

(b) Bond Angles

Ru(2)–Ru(1)–Ru(3)	59.54 (2)	Ru(2)–Ru(1)–P	110.98 (5)
Ru(2)–Ru(1)–C(1)	95.2 (3)	Ru(2)—Ru(1)–C(2)	148.7 (3)
Ru(2)–Ru(1)–C(8)	74.1 (2)	Ru(2)–Ru(1)–C(9)	46.1 (2)
Ru(3)–Ru(1)–P	51.46 (5)	Ru(3)–Ru(1)–C(1)	95.4 (3)
Ru(3)–Ru(1)—C(2)	149.5 (3)	Ru(3)–Ru(1)–C(8)	90.1 (2)
Ru(3)–Ru(1)–C(9)	58.4 (2)	P–Ru(1)–C(1)	90.0 (3)
P–Ru(1)–C(2)	99.3 (3)	P–Ru(1)–C(8)	105.5 (2)
P–Ru(1)–C(9)	94.3 (2)	C(1)–Ru(1)–C(2)	92.6 (4)
C(1)–Ru(1)–C(8)	163.4 (4)	C(1)–Ru(1)–C(9)	139.7 (3)
C(2)–Ru(1)–C(8)	90.6 (4)	C(2)–Ru(1)–C(9)	126.0 (4)
C(8)–Ru(1)–C(9)	35.6 (3)	Ru(1)–Ru(2)–Ru(3)	62.97 (2)
Ru(1)–Ru(2)–C(3)	67.9 (3)	Ru(1)–Ru(2)–C(4)	114.6 (3)
Ru(1)–Ru(2)–C(5)	141.3 (3)	Ru(1)–Ru(2)–C(9)	57.1 (2)
Ru(1)–Ru(2)–C(12)	111.9 (2)	Ru(3)–Ru(2)–C(3)	130.1 (3)
Ru(3)–Ru(2)–C(4)	102.4 (3)	Ru(3)–Ru(2)–C(5)	133.1 (3)
Ru(3)–Ru(2)–C(9)	63.0 (2)	Ru(3)–Ru(2)–C(12)	50.5 (2)
C(3)–Ru(2)–C(4)	89.9 (5)	C(3)–Ru(2)–C(5)	91.6 (5)
C(3)–Ru(2)–C(9)	97.2 (4)	C(3)–Ru(2)–C(12)	176.3 (4)
C(4)–Ru(2)–C(5)	97.1 (5)	C(4)–Ru(2)–C(9)	165.0 (4)
C(4)–Ru(2)–C(12)	93.4 (4)	C(5)–Ru(2)–C(9)	95.9 (4)
C(5)–Ru(2)–C(12)	86.5 (4)	C(9)–Ru(2)–C(12)	79.9 (3)
Ru(1)–Ru(3)–Ru(2)	57.50 (2)	Ru(1)–Ru(3)–P	49.22 (5)
Ru(1)–Ru(3)–C(6)	91.2 (3)	Ru(1)–Ru(3)–C(7)	140.6 (3)
Ru(1)–Ru(3)–C(10)	80.4 (2)	Ru(1)–Ru(3)–C(11)	109.3 (2)
Ru(1)–Ru(3)–C(12)	104.1 (2)	Ru(2)–Ru(3)–P	106.71 (5)
Ru(2)–Ru(3)–C(6)	87.3 (3)	Ru(2)–Ru(3)–C(7)	161.8 (3)
Ru(2)–Ru(3)–C(10)	70.8 (2)	Ru(2)–Ru(3)–C(11)	70.4 (2)
Ru(2)–Ru(3)–C(12)	48.0 (2)	P–Ru(3)–C(6)	96.7 (3)
P–Ru(3)–C(7)	91.4 (3)	P–Ru(3)–C(10)	97.1 (2)
P–Ru(3)–C(11)	133.5 (2)	P–Ru(3)–C(12)	151.8 (2)
C(6)–Ru(3)–C(7)	93.4 (4)	C(6)–Ru(3)–C(10)	157.8 (3)
C(6)–Ru(3)–C(11)	132.2 (3)	C(6)–Ru(3)–C(12)	97.4 (3)
C(7)–Ru(3)C(10)	106.2 (4)	C(7)–Ru(3)–C(11)	96.2 (4)
C(7)–Ru(3)–C(12)	114.1 (4)	C(10)–Ru(3)–C(11)	36.9 (3)
C(10)–Ru(3)–C(12)	65.4 (3)	C(11)–Ru(3)–C(12)	36.8 (3)
Ru(1)–P–Ru(3)	79.32 (5)	Ru(1)–P–C(28)	117.4 (3)
Ru(1)–P–C(34)	118.8 (3)	Ru(3)–P–C(28)	118.5 (3)
Ru(3)–P–C(34)	121.1 (3)	C(28)–P–C(34)	102.1 (4)
Ru(1)–C(1)–O(1)	176.1 (4)	Ru(1)–C(2)–O(2)	175.8 (4)
Ru(2)–C(3)–O(3)	167.3 (5)	Ru(2)–C(4)–O(4)	177.0 (5)
Ru(2)–C(5)–O(5)	177.7 (5)	Ru(3)–C(6)–O(6)	177.3 (4)
Ru(3)–C(7)–O(7)	174.9 (4)	Ru(1)–C(8)–C(9)	77.6 (3)
Ru(1)–C(9)–Ru(2)	76.8 (2)	Ru(1)–C(9)–C(8)	66.8 (4)
Ru(1)–C(9)–C(10)	120.5 (3)	Ru(2)–C(9)–C(8)	122.0 (4)
Ru(2)–C(9)–C(10)	114.8 (3)	C(8)–C(9)–C(10)	122.3 (5)
Ru(3)–C(10)–C(9)	86.1 (3)	Ru(3)–C(10)–C(11)	71.0 (3)
Ru(3)–C(10)–C(13)	125.6 (3)	C(9)–C(10)–C(11)	112.2 (5)
C(9)–C(10)–C(13)	118.3 (5)	C(11)–C(10)–C(13)	127.2 (5)
Ru(3)–C(11)–C(10)	72.1 (3)	Ru(3)–C(11)–C(12)	69.6 (3)
Ru(3)–C(11)–C(16)	129.7 (3)	C(10)–C(11)–C(12)	116.6 (5)
C(10)–C(11)–C(16)	123.4 (5)	C(12)–C(11)–C(16)	120.1 (5)
Ru(2)—C(12)–Ru(3)	81.5 (2)	Ru(2)–C(12)–C(11)	112.9 (3)
Ru(2)–C(12)–C(22)	120.4 (4)	Ru(3)–C(12)–C(11)	73.6 (3)
Ru(3)–C(12)–C(22)	130.2 (3)	C(11)–C(12)–C(22)	123.4 (5)
C(10)–C(13)–C(14)	108.6 (5)	C(10)–C(13)–C(15)	115.0 (5)
C(14)–C(13)–C(15)	111.4 (5)		

[a] Corresponding parameters for molecule B are listed in Table S8.

Table IV. Important Bond Lengths (Å) and Angles (deg) fo $Ru_3(CO)_7\{\mu_3\text{-}\eta^5\text{-}CH_2CC(i\text{-}Pr)C(i\text{-}Pr)C(i\text{-}Pr)C(Me)\}(\mu\text{-}PPh_2)$ (8)

(a) Bond Lengths

Ru(1)–Ru(2)	2.8633 (4)	Ru(1)–Ru(3)	2.8398 (4)
Ru(1)–P	2.284 (1)	Ru(1)–C(1)	1.869 (5)
Ru(1)–C(2)	1.870 (5)	Ru(1)–C(8)	2.285 (5)
Ru(1)–C(9)	2.173 (4)	Ru(2)–Ru(3)	2.8123 (4)
Ru(2)–C(3)	1.965 (5)	Ru(2)–C(4)	1.902 (4)
Ru(2)–C(5)	1.931 (5)	Ru(2)–C(9)	2.080 (4)
Ru(2)–C(12)	2.124 (4)	Ru(3)–P	2.323 (1)
Ru(3)–C(6)	1.883 (5)	Ru(3)–C(7)	1.877 (5)
Ru(3)–C(10)	2.460 (4)	Ru(3)–C(11)	2.263 (4)
Ru(3)–C(12)	2.168 (4)	P–C(20)	1.829 (4)
P–C(26)	1.828 (4)	C(1)–O(1)	1.135 (6)
C(2)–O(2)	1.134 (6)	C(3)–O(3)	1.127 (6)
C(4)–O(4)	1.120 (6)	C(5)–O(5)	1.126 (7)
C(6)–O(6)	1.137 (6)	C(7)–O(7)	1.130 (6)
C(8)–C(9)	1.392 (6)	C(9)–C(10)	1.471 (6)
C(10)–C(11)	1.459 (6)	C(10)–C(14)	1.538 (6)
C(11)–C(12)	1.402 (6)	C(11)–C(17)	1.543 (7)
C(12)–C(13)	1.520 (7)	C(14)–C(15)	1.534 (7)
C(14)–C(16)	1.526 (8)	C(17)–C(18)	1.551 (9)
C(17)–C(19)	1.532 (9)		

(b) Bond Angles

Ru(2)–Ru(1)–Ru(3)	59.09 (1)	Ru(2)–Ru(1)–P	89.66 (2)
Ru(2)–Ru(1)–C(1)	106.2 (1)	Ru(2)–Ru(1)–C(2)	162.1 (1)
Ru(2)–Ru(1)–C(8)	72.8 (1)	Ru(2)–Ru(1)–C(9)	46.3 (1)
Ru(3)–Ru(1)–P	52.57 (2)	Ru(3)–Ru(1)–C(1)	149.9 (1)
Ru(3)–Ru(1)–C(2)	111.9 (1)	Ru(3)–Ru(1)–C(8)	107.0 (1)
Ru(3)–Ru(1)–C(9)	71.4 (1)	P–Ru(1)–C(1)	105.5 (1)
P–Ru(1)–C(2)	96.2 (1)	P–Ru(1)–C(8)	158.8 (1)
P–Ru(1)–C(9)	122.5 (1)	C(1)–Ru(1)–C(2)	88.6 (2)
C(1)–Ru(1)–C(8)	91.1 (2)	C(1)–Ru(1)–C(9)	119.4 (2)
C(2)–Ru(1)–C(8)	97.4 (2)	C(2)–Ru(1)–C(9)	117.6 (2)
C(8)–Ru(1)–C(9)	36.3 (2)	Ru(1)–Ru(2)–Ru(3)	60.04 (1)
Ru(1)–Ru(2)–C(3)	117.5 (1)	Ru(1)–Ru(2)–C(4)	142.2 (1)
Ru(1)–Ru(2)–C(5)	76.4 (1)	Ru(1)–Ru(2)–C(9)	49.1 (1)
Ru(1)–Ru(2)–C(12)	101.5 (1)	Ru(3)–Ru(2)–C(3)	90.3 (1)
Ru(3)–Ru(2)–C(4)	134.7 (1)	Ru(3)–Ru(2)–C(5)	130.6 (1)
Ru(3)–Ru(2)–C(9)	73.2 (1)	Ru(3)–Ru(2)–C(12)	49.7 (1)
C(3)–Ru(2)–C(4)	98.7 (2)	C(3)–Ru(2)–C(5)	90.2 (2)
C(3)–Ru(2)–C(9)	162.5 (2)	C(3)–Ru(2)–C(12)	94.6 (2)
C(4)–Ru(2)–C(5)	93.9 (2)	C(4)–Ru(2)–C(9)	97.2 (2)
C(4)–Ru(2)–C(12)	85.1 (2)	C(5)–Ru(2)–C(9)	96.1 (2)
C(5)–Ru(2)–C(12)	175.1 (2)	C(9)–Ru(2)–C(12)	79.3 (2)
Ru(1)–Ru(3)–Ru(2)	60.87 (1)	Ru(1)–Ru(3)–P	51.34 (2)
Ru(1)–Ru(3)–C(6)	118.8 (1)	Ru(1)–Ru(3)–C(7)	136.2 (1)
Ru(1)–Ru(3)–C(10)	62.7 (1)	Ru(1)–Ru(3)–C(11)	95.9 (1)
Ru(1)–Ru(3)–C(12)	101.1 (1)	Ru(2)–Ru(3)–P	90.15 (2)
Ru(2)–Ru(3)–C(6)	170.7 (1)	Ru(2)–Ru(3)–C(7)	97.8 (1)
Ru(2)–Ru(3)–C(10)	67.6 (1)	Ru(2)–Ru(3)–C(11)	71.4 (1)
Ru(2)–Ru(3)–C(12)	48.4 (1)	P–Ru(3)–C(6)	96.3 (1)
P–Ru(3)–C(7)	94.9 (1)	P–Ru(3)–C(10)	112.6 (1)
P–Ru(3)–C(11)	147.2 (1)	P–Ru(3)–C(12)	138.2 (1)
C(6)–Ru(3)–C(7)	88.3 (2)	C(6)–Ru(3)–C(10)	103.6 (2)
C(6)–Ru(3)–C(11)	99.8 (2)	C(6)–Ru(3)–C(12)	125.5 (2)
C(7)–Ru(3)–C(10)	148.2 (2)	C(7)–Ru(3)–C(11)	113.8 (2)
C(7)–Ru(3)–C(12)	86.9 (2)	C(10)–Ru(3)–C(11)	35.7 (1)
C(10)–Ru(3)–C(12)	62.1 (1)	C(11)–Ru(3)–C(12)	36.8 (1)
Ru(1)–P–Ru(3)	76.10 (2)	Ru(1)–P–C(20)	119.1 (1)
Ru(1)–P–C(26)	121.8 (1)	Ru(3)–P–C(20)	121.2 (1)
Ru(3)–P–C(26)	117.0 (1)	C(20)–P–C(26)	101.9 (2)
Ru(1)–C(1)–O(1)	178.6 (2)	Ru(1)–C(2)–O(2)	178.2 (2)
Ru(2)–C(3)–O(3)	178.2 (2)	Ru(2)–C(4)–O(4)	178.9 (2)
Ru(2)–C(5)–O(5)	173.6 (2)	Ru(3)–C(6)–O(6)	176.2 (2)
Ru(3)–C(7)–O(7)	177.9 (2)	Ru(1)–C(8)–C(9)	67.5 (2)
Ru(1)–C(9)–Ru(2)	84.6 (1)	Ru(1)–C(9)–C(8)	76.3 (2)
Ru(1)–C(9)–C(10)	97.4 (1)	Ru(2)–C(9)–C(8)	124.5 (2)
Ru(2)–C(9)–C(10)	111.1 (1)	C(8)–C(9)–C(10)	122.7 (2)
Ru(3)–C(10)–C(9)	95.1 (1)	Ru(3)–C(10)–C(11)	64.8 (2)
Ru(3)–C(10)–C(14)	126.8 (2)	C(9)–C(10)–C(11)	114.0 (2)
C(9)–C(10)–C(14)	117.9 (2)	C(11)–C(10)–C(14)	124.2 (2)
Ru(3)–C(11)–C(10)	79.5 (2)	Ru(3)–C(11)–C(12)	67.9 (2)
Ru(3)–C(11)–C(17)	128.7 (2)	C(10)–C(11)–C(12)	113.9 (2)
C(10)–C(11)–C(17)	121.0 (3)	C(12)C(11)–C(17)	124.4 (3)
Ru(2)–C(12)–Ru(3)	81.9 (1)	Ru(2)–C(12)–C(11)	114.7 (2)
Ru(2)–C(12)–C(13)	119.9 (2)	Ru(3)–C(12)–C(11)	75.3 (2)
Ru(3)–C(12)–C(13)	126.8 (2)	C(11)–C(12)–C(13)	122.9 (3)
C(10)–C(14)–C(15)	111.5 (3)	C(10–C(14)–C(16)	116.2 (3)
C(15)–C(14)–C(16)	112.5 (3)	C(11)–C(17)–C(18)	108.3 (3)
C(11)–C(17)–C(19)	117.5 (3)	C(18)–C(17)–C(19)	109.7 (4)

Scheme I

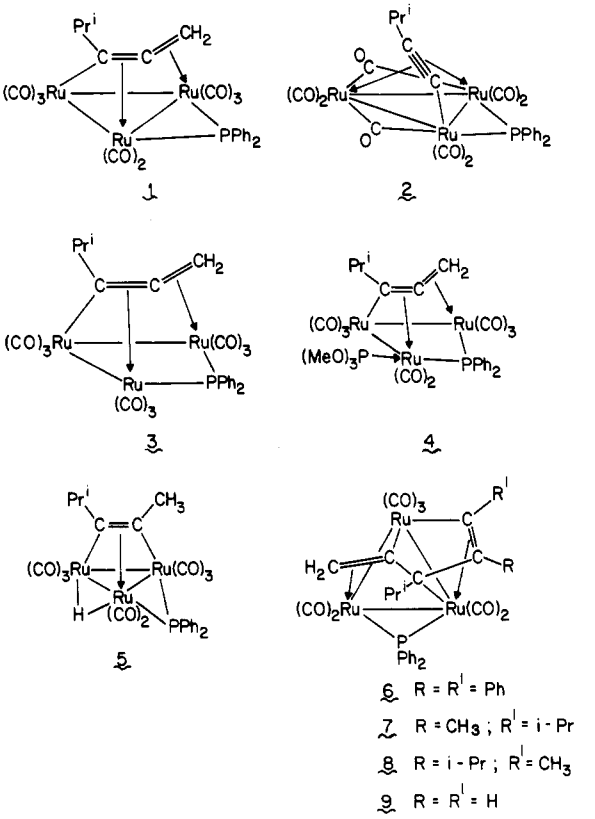

mits only one possibility for the structure of 3 (Scheme I). The molecule is a 50 electron cluster having three terminal carbonyls attached to each ruthenium, an allenyl ligand bound in the same fashion as in 1, and a phosphido bridge across an open edge. Whether or not the phosphido bridge occupies axial or equatorial sites[1] cannot be determined at this time. There is likely to be a substantial difference in the ^{31}P NMR shifts of such isomers; however, we do not as yet have sufficient data to establish a definite correlation between ^{31}P NMR chemical shifts and the stereochemical disposition of phosphido bridges.

The reversible nature of the carbonylation of 1, as depicted in eq 1, is analogous to the closely related acetylide system (eq 2) with the major differences being that the

$$Ru_3(CO)_8\{\mu_3\text{-}\eta^3\text{-}CH_2CC(i\text{-}Pr)\}(\mu\text{-}PPh_2) + CO \rightleftharpoons Ru_3(CO)_9\{\mu_3\text{-}\eta^3\text{-}CH_2CC(i\text{-}Pr)\}(\mu\text{-}PPh_2) \quad (1)$$

$$Ru_3(CO)_6(\mu\text{-}CO)_2\{\mu_3\text{-}\eta^2\text{-}CC(i\text{-}Pr)\}(\mu\text{-}PPh_2) + CO \rightleftharpoons Ru_3(CO)_9\{\mu_3\text{-}\eta^2\text{-}CC(i\text{-}Pr)\}(\mu\text{-}PPh_2) \quad (2)$$

arrangement of the acetylide in $Ru_3(CO)_6(\mu\text{-}CO)_2\{\mu_3\text{-}\eta^2\text{-}CC(i\text{-}Pr)\}(\mu\text{-}PPh_2)$ is not the same as the allenyl ligand in $Ru_3(CO)_8\{\mu_3\text{-}\eta^3\text{-}CH_2CC(i\text{-}Pr)\}(\mu\text{-}PPh_2)$ and bridging CO's in the former are absent in the latter. In both cases the forward reaction is much more rapid than the reverse (i.e., carbonylation is complete in a matter of seconds whereas decarbonylation requires a nitrogen purge through gently heated solutions for a period of several hours). The ^{31}P NMR shifts of these carbonylated 50-electron clusters differ by ca. 50 ppm, a fact which may be ascribed to the presence of different hydrocarbyl ligands, to differences in the axial or equatorial nature of the phosphido bridge relative to the Ru_3 skeleton or to a combination of these effects. Differences of ca. 30 ppm in $\delta(^{31}P)$ have been found for axial and equatorial PPh_2 isomers in acetylene insertion products described later in this paper.

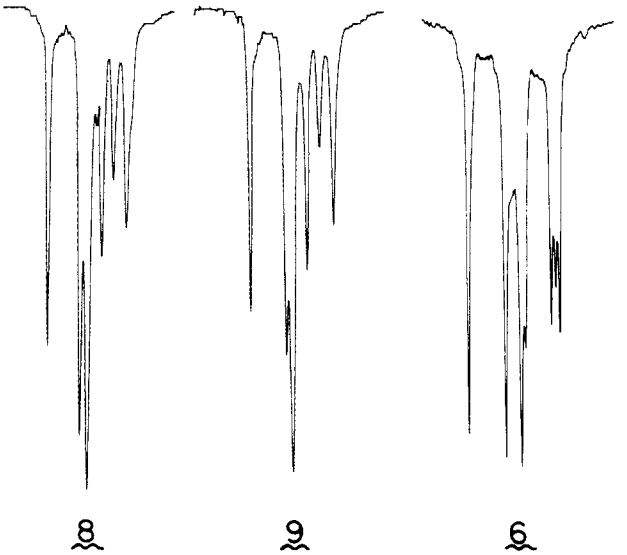

Figure 2. The ν(CO) IR spectra of $Ru_3(CO)_7\{\mu_3\text{-}\eta^5\text{-}CH_2CC(i\text{-}Pr)C(i\text{-}Pr)C(CH_3)\}(\mu\text{-}PPh_2)$ (**8**), $Ru_3(CO)_7\{\mu_3\text{-}\eta^5\text{-}CH_2CC(i\text{-}Pr)C(H)C(H)\}(\mu\text{-}PPh_2)$ (**9**), and $Ru_3(CO)_7\{\mu_3\text{-}\eta^5\text{-}CH_2CC(i\text{-}Pr)C(Ph)C(Ph)\}(\mu\text{-}PPh_2)$ (**6**) in C_6H_{12}.

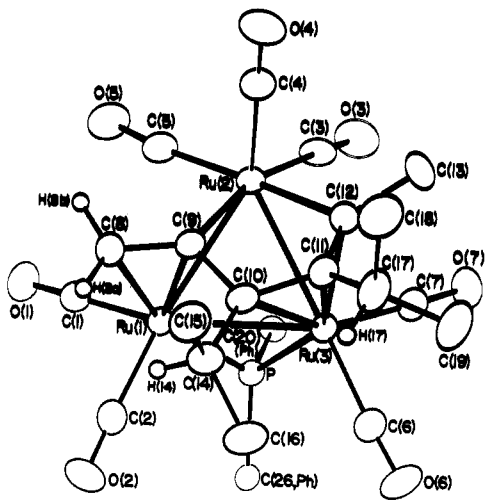

Figure 3. An ORTEP plot of the molecular structure of $Ru_3(CO)_7\{\mu_3\text{-}\eta^5\text{-}CH_2CC(i\text{-}Pr)C(i\text{-}Pr)C(CH_3)\}(\mu\text{-}PPh_2)$ (**8**) showing the atomic numbering.

Phosphite Addition to 1. In a manner similar to that for CO, addition of $P(OMe)_3$ to solutions of **1** results in a rapid color change from maroon to yellow. The ^{31}P NMR data show the presence of two doublets at 135.9 and −7.2 ppm with J_{PP} = 314 Hz. The low-field signal is assigned to the phosphite and the high-field resonance to the phosphido bridge, an assignment confirmed by a undecoupled spectrum. Using arguments similar to those for the reaction of **1** with CO the likely structure for **4** has a phosphido bridge across a nonbonded metal edge trans to the $P(OMe)_3$ ligand.

Alkyne Addition to 1. The general reaction of **1** with alkynes involves insertion into a Ru–C σ-bond, loss of CO, and extension of the cluster bound hydrocarbyl chain from three to five atoms (eq 3).

$$Ru_3(CO)_8\{\mu_3\text{-}\eta^3\text{-}CH_2CC(i\text{-}Pr)\}(\mu\text{-}PPh_2) + RC{\equiv}CR' \rightarrow Ru_3(CO)_7\{\mu_3\text{-}\eta^5\text{-}CH_2CC(i\text{-}Pr)C(R)C(R')\}(\mu\text{-}PPh_2) + CO \quad (3)$$

The reactions of **1** with MeC≡C(*i*-Pr) and HC≡CH gave what appeared to be the same type of insertion product as indicated by similarities in color, IR spectra, and R_f values. Surprisingly, the major product from the reaction with PhC≡CPh was a compound having a markedly different color (red as opposed to light orange), smaller R_f value, and quite different ν(CO) spectrum (Figure 2). Structural differences between the two types of compound were revealed by single-crystal X-ray analyses.

Crystal Structure of 8. The structure of **8** is depicted by the ORTEP II plot shown in Figure 3. The three metal atoms define a closed triangle with normal Ru–Ru bond lengths ranging from 2.8123 (4) for Ru(2)–Ru(3) to 2.8633 (4) Å for Ru(1)–Ru(2). All carbonyl ligands are terminal although the CO group C(5)–O(5) shows a slight bending at C(5) (Ru(2)–C(5)–O(5) = 173.6 (2)°) possibly suggesting a semibridging CO group. However the Ru(1)···C(5) distance is very long at 3.85 Å, and there is probably little interaction between these two atoms. The PPh_2 group occupies axial sites on Ru(1) and Ru(3) unlike the situation in its precursor, **1**, and forms two strong Ru–P bonds with distances Ru(1)–P = 2.284 (1) Å and Ru(3)–P = 2.323 (1) Å and an angle at phosphorus of Ru(1)–P–Ru(3) = 76.10 (2)°.

The hydrocarbon is bonded to the cluster face via carbon atoms C(8) through C(12). Bond lengths and angles associated with this fragment suggest a C(8)–C(9) double bond (1.392 (6) Å) interacting in π-fashion with Ru(1) and a C(9)–Ru(2) σ-interaction (2.080 (4) Å). The C(9)–C(10) and C(10)–C(11) bond lengths of 1.471 (6) Å and 1.459 (6) Å, respectively, are significantly shorter than a C–C single bond (1.54 Å)[7] but longer than a C–C double bond (1.34 Å),[7] suggesting that some multiple-bond character is delocalized over these three carbon atoms. The C(11)–C(12) distance of 1.402 (6) Å is consistent with a double bond interacting in π-fashion with Ru(3). Finally the distance of 2.124 (4) Å between Ru(2) and C(12) suggests a σ-type interaction.

Comparison with the structure of the precursor **1**[1] shows that insertion of MeC≡C(*i*-Pr) into the C(11)–Ru(2) bond of **1** has occurred generating a carbon–carbon bond between the C(*i*-Pr) unit of **1** and the alkyne carbon. The stereochemistry at the newly formed [C(10)–C(11)] carbon–carbon bond of **8** (R = *i*-Pr, R′ = Me) is cis, and the atoms Ru(2), C(9), C(10), C(11) and C(12) form a five-membered delocalized metallacycle η-coordinated to Ru(3). It seems likely that the stereochemistry of the insertion is dictated by the favorable coordinating characteristics of a "wrap-around" chain coupled with steric constraints. A trans arrangement of the substituents on C(10) and C(11) would place the isopropyl group on C(11) in repulsive contact with $Ru(2)(CO)_3$.

Knox and co-workers[8] have recently suggested that the stereochemistry of a growing carbon chain in alkyne oligomerization[9] initiated by μ-alkylidene compounds is controlled by steric factors and indeed have isolated a binuclear ruthenium complex with a "wrap around" five-carbon chain related to that in **8**.

The five carbon atoms in the hydrocarbon chain of **8** are derived from an acetylide, a methylene group, and an alkyne. If the cluster-bound acetylide is regarded as an

(7) *Molecular Structures and Dimensions*; Kennard, O., Watson, D. G., Allen, F. H., Isaacs, N. W., Motherwell, W. D. S., Petterson, R. C., Town, W. G., Eds.; N. V. A. Oosthoek: Utrecht, 1976; Vol. A1.

(8) Adams, P. Q.; Davies, D. L.; Dyke, A. F.; Knox, S. A. R.; Mead, K. A.; Woodward, P. *J. Chem. Soc., Chem. Commun.* **1983**, 222.

(9) See also: Levisalles, J.; Rose-Munch, F.; Rudler, H.; Daran, J. C.; Dromzee, Y.; Jeannin, Y.; Ades, D.; Fontanille, M. *J. Chem. Soc. Chem. Commun.* **1981**, 1055.

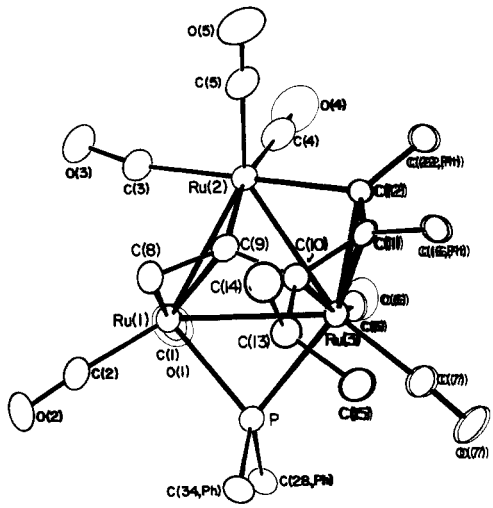

Figure 4. The molecular structure of $Ru_3(CO)_7\{\mu_3\text{-}\eta^5\text{-}CH_2CC(i\text{-}Pr)C(Ph)C(Ph)\}(\mu\text{-}PPh_2)$ (6).

alkylidyne carbide, as has been suggested,[10] the components of the chain are a carbido carbon, an alkylidyne (CR), an alkylidene (CH_2), and an alkyne. All of these fragments have been invoked as possible surface-bound species in hydrocarbon chain growth in Fischer–Tropsch catalysis,[11] and most recently coupling of alkylidyne and alkyne species to form 1,3-dimetallaallyl fragments has been proposed.[12] The molecule 8 can be seen as a model for chain growth involving three of the C(1) units (C, CH, CH_2) thought to be present on surfaces in the Fischer–Tropsch process and is illustrative of the potentially wide variety of structural units which could be assembled from C(1) species.

Crystal Structure of 6. Slow crystallization of the product of the reaction between 1 and PhC≡CPh from benzene produced dark red prisms of 6 (R = R′ = Ph). The cluster crystallizes in the acentric space group $P2_1$ and contains two crystallographically independent molecules in the asymmetric unit. Except for minor differences in bond lengths and angles the two molecules A and B are essentially identical. Discussion of the structure will be centered about molecule A with corresponding values for B appearing in parentheses.

The structure of 6 resembles that of 8 (vide infra) in many respects, but there are some marked geometrical differences and more subtle changes in the bonding of the unsaturated chain. A compilation of significant bond lengths and angles is presented in Table III with an ORTEP II plot of the structure of 6 in Figure 4. The first notable difference from 8 is the disposition of the phosphido bridge which occupies equatorial sites in 6 with the phosphorus atom coplanar with the Ru_3 triangle. The stereochemistry of the phosphido bridges in 6 and 8 relative to the metal plane is better illustrated in Figure 5 which is a view down the Ru(1)–Ru(3) bond of each cluster. The μ-PPh_2 group is not precisely at right angles to the plane of the metal atoms in 8; an angle of 117° is defined by the planes Ru-

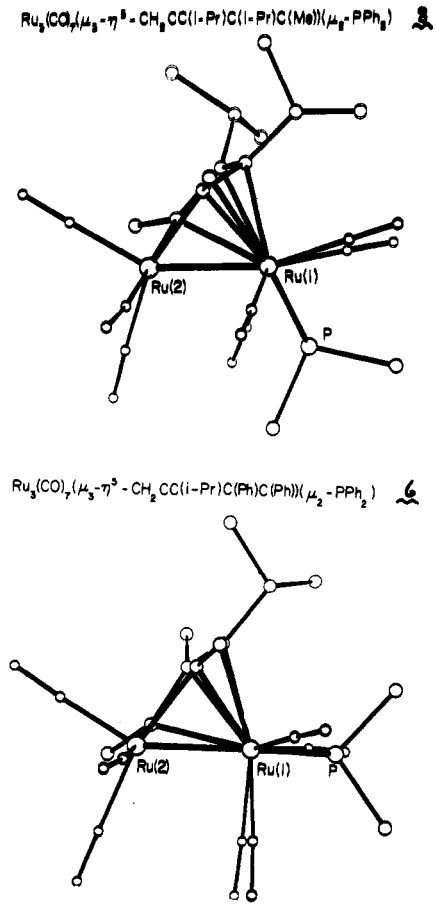

Figure 5. A comparison of the molecular structures of 8 and 6 viewed along the Ru(1)–Ru(3) bond. The ball and stick drawings emphasize the dispositions of the μ-PPh_2 groups relative to the Ru_3 plane in the two cases.

(1)–Ru(2)–Ru(3) and Ru(1)–P–Ru(3). The change from an equatorial μ-PPh_2 group in 6 to an axial configuration in 8 appears to require a concomitant rearrangement of the carbonyl groups to accommodate the phosphido bridge. Thus while two carbonyl groups are trans to Ru(2) in 8 (Ru(2)–Ru(1)–C(2) = 162.1 (1)°; Ru(2)–Ru(3)–C(6) = 170.6 (1)°), none are trans to Ru(2) in 6. The similarity between 6 and 8 extends to the presence of a carbonyl group in each cluster (C(5)–O(5) in 8; C(3)–O(3) in 6) with semibridging characteristics. The semibridging interaction is stronger in 6 (Ru(2)–C(3)–O(3) = 167.3 (5)°; Ru(1)···C(3) = 2.719 (11) Å) than in 8. Differences in the bonding of the hydrocarbon appear to be centered mainly about C(10) and may be due to the electron-donating (*i*-Pr, Me) or -attracting (Ph) character of the groups on the alkyne or to steric interactions between the C(10) isopropyl group and the phosphido bridge phenyl ring as a result of the differing stereochemistry of the μ-PPh_2 ligands in 6 and 8. In the structure of 8 (R = *i*-Pr, R′ = Me) the distances C(10)–C(9) = 1.471 (6) Å and C(10)–C(11) = 1.459 (6) Å seem to indicate that some multiple-bond character is distributed over these three atoms while in 6 (R = R′ = Ph) the distances C(10)–C(9) = 1.488 (12) (1.489 (2)) Å and C(10)–C(11) = 1.438 (12) (1.455 (12)) Å show that the multiple-bond character is restricted mainly to C(10)–C(11). Secondly, the Ru(3)–C(10) interaction is much shorter in the diphenylacetylene derivative (2.279 (8) Å) than in the methylisopropylacetylene insertion product (2.460 (4) Å). Attainment of a 48-electron count requires that the organic ligand donates seven electrons to the metals. This could be visualized as being achieved by a C(8)–C(9) π-bond (two electrons), a C(9)–Ru(2) σ-bond (one electron), a C(12)–

(10) (a) Carty, A. J. *Pure Appl. Chem.* **1982**, *54*, 113. (b) Halet, J. F.; Saillard, J. Y.; McGlinchey, M. J.; Jaouen, G. *Inorg. Chem.* **1985**, *24*, 1695. (c) Nucciarone, D.; Taylor, N. J.; Carty, A. J. *Organometallics* **1986**, *5*, 1179.

(11) (a) Muetterties, E. L.; Rhodin, T. N.; Band, E.; Bruder, C. F.; Pretzer, W. R. *Chem. Rev.* **1979**, *79*, 91. (b) Rofer-DePoorter, C. K. *Chem. Rev.* **1981**, *81*, 447.

(12) Beanan, L. R.; Keister, J. B. *Organometallics* **1985**, *4*, 1713 and references therein.

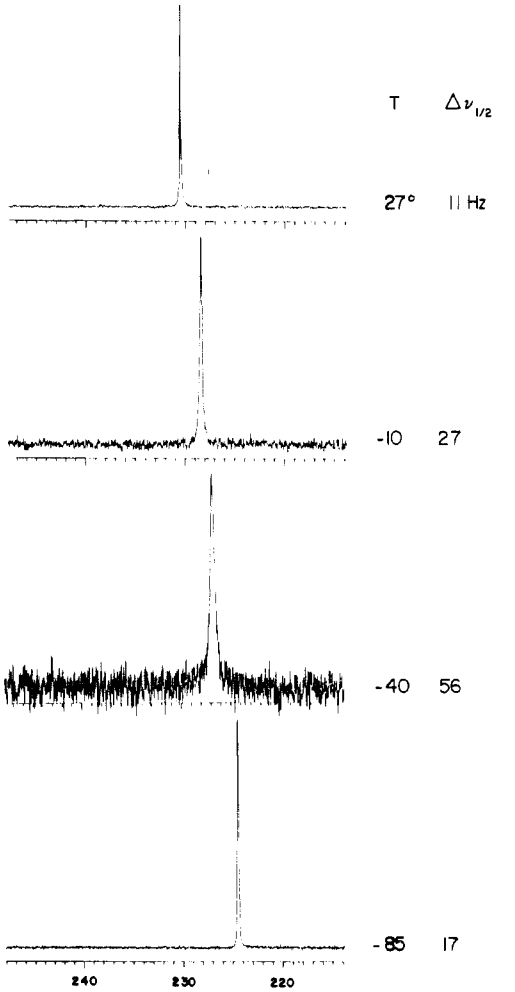

Figure 6. The variable-temperature $^{31}P\{^1H\}$ NMR spectra of $Ru_3(CO)_7\{\mu_3\text{-}\eta^5\text{-}CH_2CC(i\text{-}Pr)C(H)C(H)\}(\mu\text{-}PPh_2)$ in CH_2Cl_2.

Ru(2) σ-bond (one electron), and a C(11)–C(12) π-bond (two electrons) giving six electrons. This leaves one-electron, which, a priori, may be assigned to a C(10)–Ru(3) σ-interaction. However examination of the bond length data shows that this C(10)–Ru(3) bond is much weaker than a normal Ru–C bond; in fact it is comparable in length to a Ru–C π-interaction. Although a better picture of the bonding nature may be provided by molecular orbital calculations, the view of a C(10)–C(11) π-type interaction with Ru(3) is perhaps more representative than a C(10)–Ru(3) σ-type interaction. Overall the tendency of the fragment C(10)–C(11)–C(12) toward a π-allyl-type interaction is more pronounced in **6** than in **8** where C(11)–C(12) has greater double-bond character.

Variable-Temperature NMR Studies of 6–9. The 250-MHz ^1H NMR spectrum of **9** (R = R′ = H) at ambient temperature consists of a series of sharp well-resolved resonances. Principal features of interest are a pair of doublets at 4.14 and 4.30 ppm due to the geminal hydrogen atoms of the methylene group and another pair of doublets at 5.64 and 8.64 ppm. The low-field signal is assigned to the hydrogen attached to the σ- and π-bound carbon atom C(12) while the higher field doublet is due to the hydrogen on C(11). It is well-known that hydrogens attached to a σ–π-vinyl-type carbon atom resonate at lower field than a hydrogen bound to an adjacent carbon atom.[13]

The $^{31}P\{^1H\}$ spectrum of **9** exhibited a single sharp line at 293 K (δ 222.2) and at 158 K (δ 217.9). Thus only one isomer appeared to be present in these solutions. However a careful study over a wide temperature range revealed that the chemical shift and the line width of the ^{31}P resonance of **9** were temperature-dependent (Figure 6) with a maximum $\Delta\nu_{1/2}$ of 56 Hz at 233 K. Similar behavior was displayed in the ^1H NMR spectra. The cluster **6** (R = R′ = Ph) also exhibited a singlet ^{31}P NMR resonance at 249.4 ppm, ~27 ppm downfield of the resonance in **9**, as do the other compounds in this series. For **6**, the X-ray analysis revealed that the phosphido group had an equatorial disposition relative to the Ru_3 plane.

For symmetrical alkynes RC≡CR coupling to the allenyl unit can give only one regioisomer of type **6**. When R ≠ R′ the alkyne can insert in two ways giving regioisomers $Ru_3(CO)_7\{\mu_3\text{-}\eta^5\text{-}CH_2CC(i\text{-}Pr)C(R)C(R')\}(\mu\text{-}PPh_2)$ and $Ru_3(CO)_7\{\mu_3\text{-}\eta^5\text{-}CH_2CC(i\text{-}Pr)C(R')C(R)\}(\mu\text{-}PPh_2)$. The ^1H and ^{31}P NMR spectra of **10** (R = Ph, R′ = H) are very similar to those of **9**. The presence of a singlet at 6.34 ppm and the lack of a singlet above 8.0 ppm shows that the hydrogen is located on C(11) and the phenyl group on C(12). Spectra of crystalline **10** showed no evidence of the other regioisomer. For the methylisopropylacetylene reaction products, $^{31}P\{^1H\}$ and ^1H NMR spectroscopy unequivocally identified two regioisomers resulting from insertion into the metal–allenyl linkage. The $^{31}P\{^1H\}$ spectra in methylene-d_2 chloride of the product of reaction between **1** and MeC≡C(*i*-Pr) at ambient temperature showed two singlets at 229.2 and 220.6 ppm, the former being broad ($\Delta\nu_{1/2}$ = 130 Hz) and the latter sharp ($\Delta\nu_{1/2}$ = 51 Hz). Variable-temperature $^{31}P\{^1H\}$ studies showed the behavior illustrated in Figure 7. On lowering the temperature the low-field resonance broadened to a maximum $\Delta\nu_{1/2}$ = 506 Hz at 263 K and then subsequently sharpened to give a narrow resonance ($\Delta\nu_{1/2}$ = 28 Hz) at 203 K. The high-field resonance exhibited similar changes, being sharp at 300 K and having a maximum half-width of 90 Hz at 243 K. These observations can be explained as follows. At room temperature the two ^{31}P resonances arise from the two alkyne insertion products $Ru_3(CO)_7\{\mu_3\text{-}\eta^5\text{-}CH_2CC(i\text{-}Pr)C(i\text{-}Pr)C(Me)\}(\mu\text{-}PPh_2)$ (**8**) and $Ru_3(CO)_7\{\mu_3\text{-}\eta^5\text{-}CH_2CC(i\text{-}Pr)C(Me)C(i\text{-}Pr)\}(\mu\text{-}PPh_2)$ (**7**) with the 220.6 ppm sharp resonance assigned to **8**. Confirmation of this assignment was provided by fractional crystallization of the mixture which gave almost pure **8**, as indicated by the ratio of intensities of the two resonances, and from which a representative single crystal, on X-ray analysis, had the structure shown in Figure 3. The variable-temperature spectra of mixtures of **7** and **8** indicate that there is no interconversion between regioisomers. Moreover the changes in chemical shifts and line widths are paralleled in the spectra of the symmetrical acetylene products **6** and **10**. The variable-temperature phenomena are consistent with a "hidden partner" exchange process.[14] This situation arises when the equilibrium between two rapidly exchanging compounds is such that one species is dominant (≥90%). As a consequence of this very unequal population situation, the minor component can be easily lost in the base line as the slow-exchange limit is approached. The

(13) (a) Henrick, K.; McPartlin, M.; Deeming, A. J.; Hasso, S.; Manning, P. *J. Chem. Soc. Dalton Trans.* **1982**, 899. (b) Aime, S.; Deeming, A. J. *J. Chem. Soc., Dalton Trans.* **1983**, 1807. (c) Nubel, P. O.; Brown, T. L. *J. Am. Chem. Soc.* **1984**, *106*, 3474. (d) Horton, A. D.; Mays, M. J.; Raithby, P. R. *J. Chem. Soc., Chem. Commun.* **1985**, 247. (e) Dyke, A. F.; Knox, S. A. R.; Morris, M. J.; Naish, P. J. *J. Chem. Soc., Dalton Trans.* **1983**, 1417. (f) Shapley, J. R.; Richter, S. I.; Tachikawa, M.; Keister, J. B. *J. Organomet. Chem.* **1975**, *94*, C43.

(14) (a) Okazawa, N.; Sorensen, T. S. *Can. J. Chem.* **1978**, *32*, 339. (b) Anet, F. A. L.; Basus, V. J. *J. Magn. Reson.* **1978**, *32*, 339.

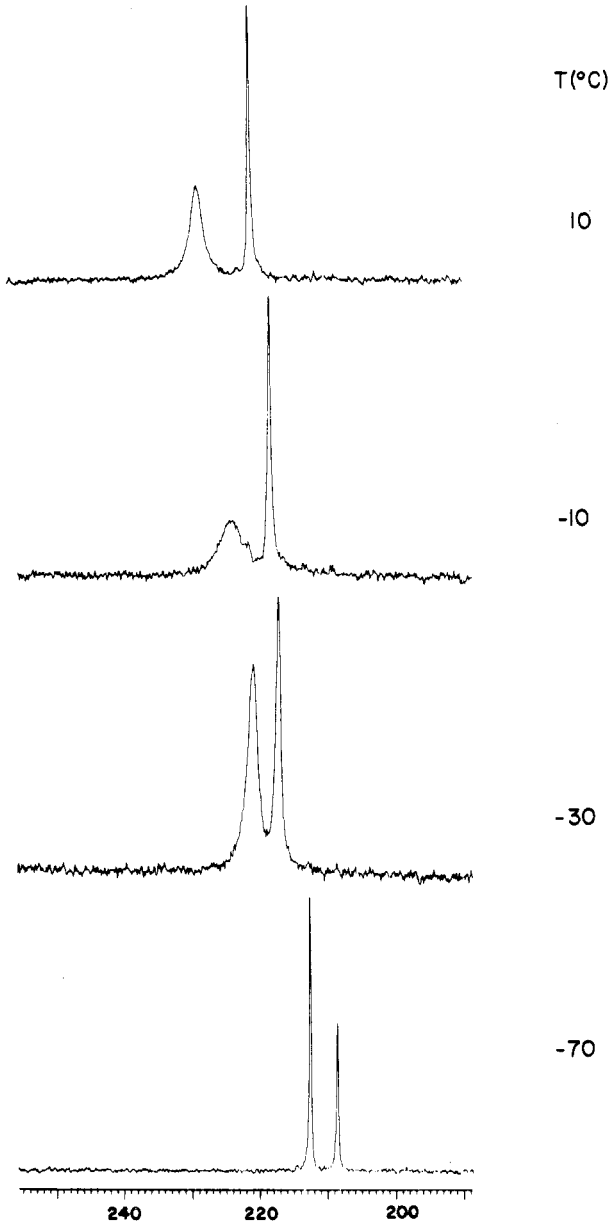

Figure 7. The variable-temperature $^{31}P\{^1H\}$ NMR spectra of a mixture of the isomers $Ru_3(CO)_7\{\mu_3\text{-}\eta^5\text{-}CH_2CC(i\text{-}Pr)C(CH_3)C(i\text{-}Pr)\}(\mu\text{-}PPh_2)$ (**7**) and $Ru_3(CO)_7\{\mu_3\text{-}\eta^5\text{-}CH_2CC(i\text{-}Pr)C(i\text{-}Pr)C(CH_3)(\mu\text{-}PPh_2)$ (**8**). The high-field resonance is due to **8**.

effect on the line shape of the major component is a broadening and subsequent sharpening as the slow-exchange limit is approached and a concurrent peak shift in the direction of the original position of the minor component by an amount proportional to the population of each.

The failure to observe the "hidden partner" may be due to either an equilibrium heavily favoring the major component, thus resulting in the resonance being lost in the baseline noise and/or a low-temperature spectrum which is not representative of the slow-exchange limit. In the latter case the minor component could have a line shape sufficiently broad enough to be lost in the base line.

Judicious choice of an appropriate disubstituted acetylene may provide a cluster in which both partners can be readily identified. Such studies are in progress.

The exchange believed to be responsible for the ^{31}P NMR observations is an axial–equatorial phosphido bridge site exchange as depicted in Scheme II. Evidence for the possible occurrence of such an exchange comes from the

Scheme II

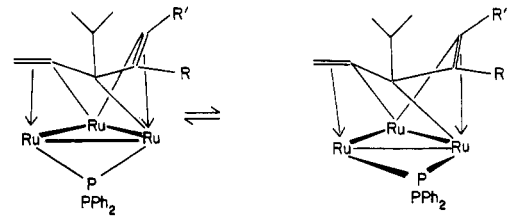

isolation and solid-state characterization of two such isomers, namely, $Ru_3(CO)_7\{\mu_3\text{-}\eta^5\text{-}CH_2CC(i\text{-}Pr)C(i\text{-}Pr)C(Me)\}(\mu\text{-}PPh_2)$ (**8**) and $Ru_3(CO)_7\{\mu_3\text{-}\eta^5\text{-}CH_2CC(i\text{-}Pr)C(Ph)C(Ph)\}(\mu\text{-}PPh_2)$ (**6**). It is significant that the ^{31}P chemical shift difference between the axial PPh_2 group in **8** and the equatorial phosphorus in **6** is ~27 ppm.

The type of exchange envisaged in Scheme II is reminiscent of the "flapping" of phosphido bridges postulated for dimers of general formula $M_2(CO)_6(\mu\text{-}PR_2)_2$.[15] In these cases exchange is believed to occur via an intermediate having a coplanar $M_2(\mu\text{-}P)_2$ skeleton and indeed cocrystallization of both planar and bent forms in the same crystal lattice have been observed.[16] Electronic and steric factors influencing the geometry of these dimers have been dealt with in detail and have been briefly summarized by Geoffroy.[16] The situation in clusters **6**–**10** is more complex since the bonding of the unsaturated ligand on the face of the cluster and steric interactions of the axial or equatorial $\mu\text{-}PPh_2$ groups with both the carbonyl ligands and the unsaturate must be considered. It is tempting to associate the preference for an axial configuration in **8** with unfavorable steric interactions between the isopropyl group on C(10) and the phenyl groups of an equatorial $\mu\text{-}PPh_2$ ligand. We are currently synthesizing a wider variety of acetylene insertion products in order to examine the possible influence of steric factors on $\mu\text{-}PPh_2$ group configurations. Axial–equatorial phosphido bridge exchange may well be an important, yet to date rarely documented feature of phosphido bridge cluster chemistry. Some recent evidence for mobility of $\mu\text{-}PR_2$ groups in clusters has indeed been gleaned from NMR measurements.[17]

Hydrogenation of 1. The reaction of **1** with molecular hydrogen was of interest not only on account of its apparent behavior as a coordinatively unsaturated molecule but also because of the possibility of obtaining information on the stepwise reduction of a multisite-bound cumulene on the face of a metal cluster. Considerable recent effort has been devoted to establishing pathways for the reduction of unsaturated hydrocarbyls (for example: alkynes,[20] carbynes,[21] nitriles,[22] alkenyls,[23] acetylides[24]) on clusters

(15) (a) Adams, R. D.; Cotton, F. A.; Cullen, W. R.; Hunter, D. L.; Mihichuk, L. *Inorg. Chem.* **1975**, *14*, 1395. (b) Flood, T. C.; Disanti, F. J.; Campbell, K. D. *Inorg. Chem.* **1978**, *17*, 1643.
(16) Harley, D. A.; Whittle, R. R.; Geoffroy, G. L. *Organometallics* **1983**, *2*, 383.
(17) Crowte, R. J.; Evans, J. *J. Chem. Soc., Chem. Commun.* **1984**, 1332.
(18) Sappa, E.; Tiripicchio, A.; Braunstein, P. *Chem. Rev.* **1983**, *83*, 203.
(19) Sappa, E.; Manotti Lanfredi, A. M.; Predieri, G.; Tiripicchio, A. *Inorg. Chim. Acta* **1982**, *61*, 217.
(20) Day, V. W.; Abdel-Meguid, S. S.; Dabestini, S.; Thomas, M. G.; Pretzer, W. R.; Muetterties, E. L. *J. Am. Chem. Soc.* **1976**, *98*, 8289.
(21) (a) Keister, J. B.; Payne, M. W.; Muscatella, M. J. *Organometallics* **1983**, *2*, 219. (b) Geoffroy, G. L.; Epstein, R. A. *Inorg. Chem.* **1977**, *16*, 2795.
(22) Andrews, M. A.; Kaesz, H. D. *J. Am. Chem. Soc.* **1979**, *101*, 7255.
(23) Burch, R. R.; Muetterties, E. L.; Teller, R. G.; Williams, J. M. *J. Am. Chem. Soc.* **1982**, *104*, 4257.
(24) Castiglioni, M.; Gervasio, G.; Sappa, E. *Inorg. Chim. Acta* **1981**, *49*, 217.

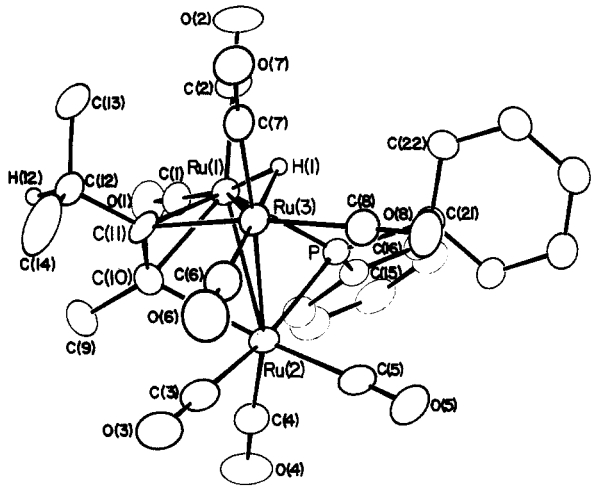

Figure 8. An ORTEP plot of the molecular structure of $(\mu\text{-H})\text{Ru}_3(\text{CO})_8\{\mu_3\text{-}\eta^2\text{-CH}_3\text{C}{\equiv}\text{C}(i\text{-Pr})\}(\mu\text{-PPh}_2)$ (**5**).

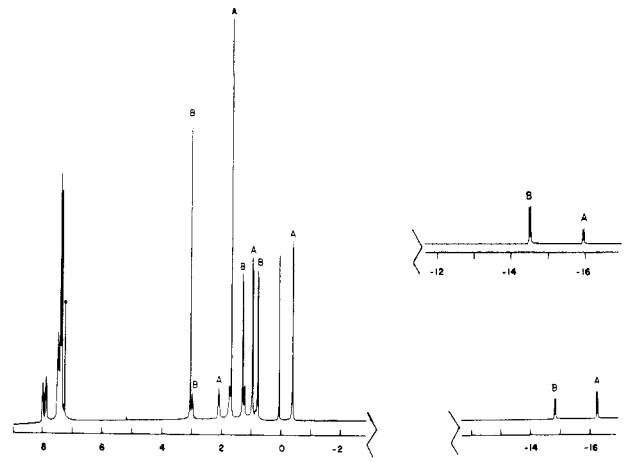

Figure 9. The ^{1}H NMR spectrum of $(\mu\text{-H})\text{Ru}_3(\text{CO})_8\{\mu_3\text{-}\eta^2\text{-CH}_3\text{C}{\equiv}\text{C}(i\text{-Pr})\}(\mu\text{-PPh}_2)$ in $CDCl_3$ at ambient temperature. Resonances due to the two isomers are labeled A and B. The inset spectrum shows the hydride region of the spectrum in C_7D_8 where the ratio of intensities is A:B = 1:2.4.

as models for such processes[25] on homogeneous and heterogeneous catalysts.

Hydrogenation of **1** proceeds rapidly at 23 °C by bubbling H_2 through a heptane solution, to give **5** in good yields. The overall reaction (eq 4) results in reduction of

$$\text{Ru}_3(\text{CO})_8(\mu_3\text{-}\eta^3\text{-CH}_2{=}\text{C}{=}\text{C}(i\text{-Pr}))(\mu\text{-PPh}_2) + \text{H}_2 \rightarrow (\mu\text{-H})\text{Ru}_3(\text{CO})_8(\mu_3\text{-}\eta^2\text{-CH}_3\text{C}_2(i\text{-Pr}))(\mu\text{-PPh}_2) \quad (4)$$

the terminal methylene to a methyl group with the other hydrogen atom ending up as a μ-hydride. This results in the conversion of a five-electron donor allenyl ligand into a four-electron donor ($2\sigma + \pi$) alkyne.

A similar hydrogenation has been reported by Castiglioni et al.[26] In their examination of the catalytic isomerization of 1-pentene to *cis*- and *trans*-2-pentene by $\text{Ru}_3(\text{CO})_{12}$ these authors were able to isolate the allenyl cluster $(\mu\text{-H})\text{Ru}_3(\text{CO})_9(\mu_3\text{-}\eta^3\text{-CH}_3\text{C(H)}{=}\text{C}{=}\text{CCH}_3)$. Hydrogenation of this cluster under cyclohexane reflux gave $(\mu\text{-H})_2\text{Ru}_3(\text{CO})_9(\mu_3\text{-}\eta^2\text{-EtC}_2\text{Me})$ plus other compounds in unreported yields. The harsh conditions required for this hydrogenation suggests prior activation of the cluster by ligand dissociation or Ru–Ru bond cleavage. The ease with which **1** is converted to **4** must be due to the presence of the phosphido bridge in **1** and the facility with which bridge opening occurs to provide active sites for incoming ligands. The facility with which **1** activates molecular hydrogen at 25 °C and 1 atm is rare for a discrete molecular cluster,[27] the only other example known to us being the recent report of Adams.[27b]

Crystal Structure of 5. Crystals of **5** were difficult to grow due to the tendency of this compound to decompose in solution. Deep red prisms suitable for X-ray diffraction studies were obtained by slow diffusion of pentane vapors into concentrated toluene solutions held at ca. −15 °C. An ORTEP II plot of the structure of **5** is found in Figure 8. Selected bond lengths and angles are found in Table II. The structure consists of an asymmetric trimetallic triangle having metal–metal distances lying within the range typically observed for trinuclear ruthenium clusters of 2.7–2.9 Å. All of the carbonyls are terminal. While the phosphido group occupied equatorial sites in **1**, it is axial in **5**. The PPh_2 group bridges the shortest cluster edge, Ru(1)–Ru(2), with Ru–P distances of 2.262 (1) and 2.420 (1) Å for Ru(1)–P and Ru(2)–P, respectively. The Ru–P–Ru angle is 72.0 (0)°, similar to that found in $\text{Ru}_2(\text{CO})_6(\mu\text{-}\eta^2\text{-C}_2(t\text{-Bu}))(\mu\text{-PPh}_2)$[10a] and $\text{Ru}_5(\text{CO})_{13}(\mu_4\text{-}\eta^2\text{-C}_2\text{Ph})(\mu\text{-PPh}_2)$[3f] of 72.0 (0)° and 72.3 (0)°, respectively. The bridging hydrogen was located across the Ru(1)–Ru(3) edge and its presence verified by ^{1}H NMR studies (vide infra).

The methylene carbon of **1** has been reduced to the methyl group labeled C(9). Consequently C(9) is no longer bound to the cluster, but the organic ligand remains attached to the Ru_3 skeleton through C(10) and C(11). The C(9)–C(10) and C(11)–C(12) distances of 1.525 (8) and 1.521 (6) Å, respectively, are normal C–C single bonds. The C(10)–C(11) distance of 1.311 (6) Å is shorter than the distance in free alkenes (1.34 Å)[7] yet substantially longer than a C–C triple bond of 1.20 Å. When compared to C–C distances of 1.37–1.44 Å observed[18] in trinuclear clusters having μ_3-coordinated alkynes, the C(10)–C(11) bond length is one of the shortest C–C distances observed for this class of compound. The Ru(2)–C(10) and Ru(3)–C(11) distances of 2.243 (5) and 2.168 (4) Å, respectively, are comparable to analogous distances in $\text{Ru}_3(\text{CO})_7\{\text{CC}(t\text{-Bu})\}(\text{PhCC(H)Ph})(\text{PhCCPh})$.[19] The C(10)–C(11) π-type interaction with Ru(1) results in bond lengths of 2.144 (5) and 2.317 (4) Å for Ru(1)–C(10) and Ru(1)–C(11), values typical of 2σ–π bound acetylenes.[18]

Spectroscopic Studies of 5. An indication that the solid-state structure determined for **5** was not entirely indicative of the solution structure arose from the IR spectrum where a weak absorption at 1864 cm^{-1} indicated the presence of a bridging carbonyl. An examination of the NMR spectral results indicate even more complex behavior. The ^{31}P NMR spectra of pure samples of **5** revealed two resonances of unequal intensity. The equilibria between these two compounds is sensitive to the choice of solvent. Thus a change of solvent from $CDCl_3$ to C_7D_8 results not only in shifts in the positions of the peaks in the ^{1}H and ^{31}P NMR spectra but also in changes in the relative concentrations of each. While the two isomers (arbitrarily labeled A and B as assigned in Figure 9) are more nearly equal in concentration to one another

(25) For reviews of metal cluster reactions and their relationship to catalysis see: (a) Deeming, A. J. In *Transition Metal Clusters*; Johnson, B. F. G., Ed.; Wiley: New York, 1980; p 391. (b) Muetterties, E. L.; Krause, M. J. *Angew. Chem., Int. Ed. Engl.* **1983**, *22*, 135.

(26) Castiglioni, M.; Milone, L.; Vaglio, G. A.; Osella, D.; Valle, M. *Inorg. Chem.* **1976**, *15*, 394.

(27) For pertinent literature see: (a) Dalton, D. M.; Barnett, D. J.; Duggan, T. P.; Keister, J. B.; Malik, P. T.; Modi, S. P.; Shaffer, M. R.; Smesko, S. A. *Organometallics* **1985**, *4*, 1854 and references therein. (b) Adams, R. D.; Wang, S. *Organometallics* **1986**, *5*, 1272.

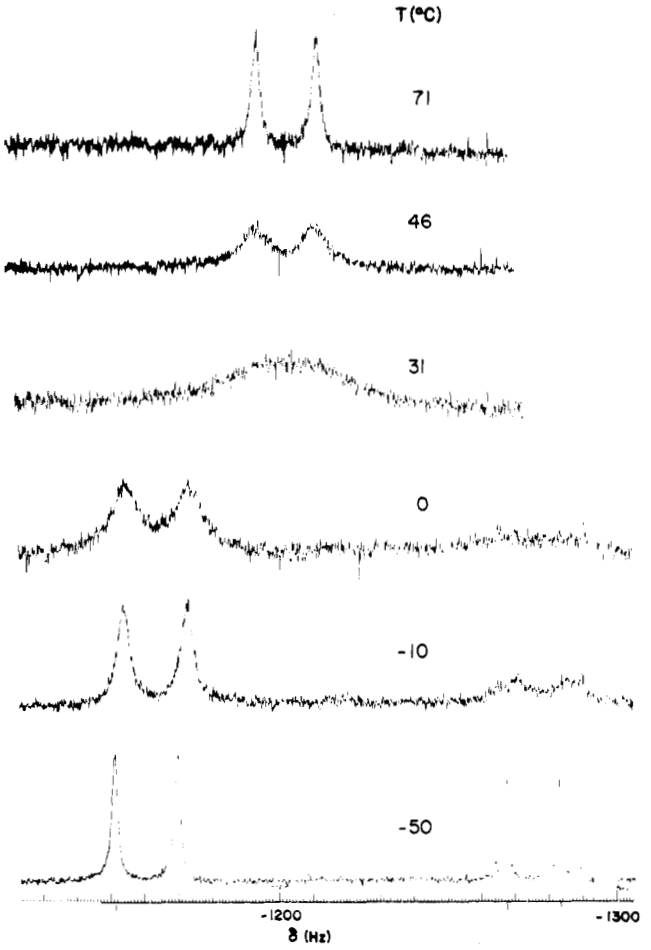

Figure 10. The variable-temperature ^1H NMR spectra of $(\mu\text{-H})Ru_3(CO)_7\{\mu_3\text{-}\eta^2\text{-}CH_3C{\equiv}C(i\text{-}Pr)\}(\mu\text{-}PPh_2)$ in the hydride region of the spectrum.

in $CDCl_3$ (ratio A:B = 1.1:1 (Figure 9)), their ratio changes in C_7D_8 to A:B = 1:2.4 (Figure 9 inset). In CD_2Cl_2 the ratio of A:B is 1.8:1.

A temperature-dependent exchange process is occurring which results in broadening and collapse of resonances due to A and B. Although high-temperature limiting spectra were not attainable for all resonances involved due to the thermal instability of **5**, pairwise collapse of the two phosphorus, μ-hydrido, isopropyl methine, isopropyl methyl, and alkenyl methyl resonances was observed in appropriate ^{31}P or ^1H spectra. Figure 10 shows these temperature effects in the hydride region of the ^1H NMR spectra. The equilibrium process responsible for these observations must include the presence of a bridging carbonyl group. Several mechanistic possibilities are consistent with these spectral results (Scheme III). These include an exchange between carbonyl-bridged and nonbridged isomers (I of Scheme III), an equilibrium involving

Scheme III

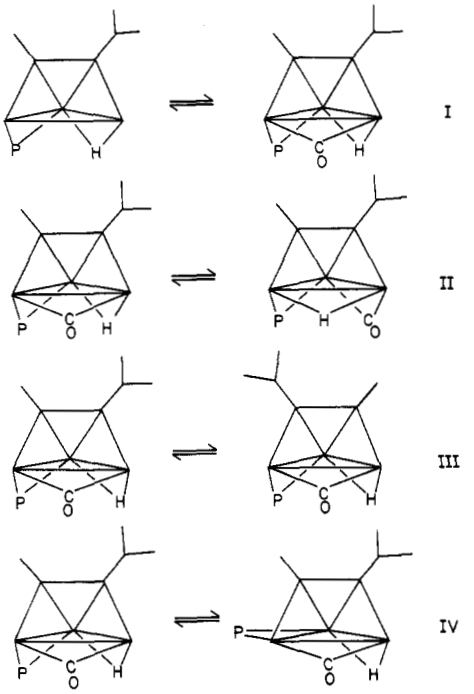

μ-CO and μ-H exchange (II), an alkyne rotation exchanging methyl and isopropyl substituents (III), and an axial–equatorial phosphido group exchange process (IV). Examples of I,[28] II,[29] and III[30] are well-established in organometallic chemistry.

Acknowledgment. We are grateful to the Natural Sciences and Engineering Research Council of Canada for financial support of this work in the form of grants (A.J.C.) and scholarships (D.N.).

Registry No. **1**, 87829-51-4; **3**, 110570-42-8; **4**, 110661-37-5; **5**, 110661-38-6; **6**, 110661-39-7; **7**, 110661-41-1; **8**, 110661-40-0; **9**, 110661-42-2; $P(OMe)_3$, 121-45-9; CO, 630-08-0; PhCCPh, 501-65-5; $i\text{-}PrCCCH_3$, 21020-27-9; HCCH, 74-86-2; Ru, 7440-18-8.

Supplementary Material Available: Tables of atomic coordinates (Tables S1–S3), anisotropic thermal parameters (Tables S4–S6), and remaining bond lengths and angles (Tables S7–S9) (16 pages); listings of structure factors (Tables S10–S12) (72 pages). Ordering information is given on any current masthead page.

(28) Aime, S.; Milone, L. *Prog. Nucl. Magn. Reson. Spectrosc.* **1977**, *11*, 183 and references therein.

(29) Rosenberg, E.; Anslyn, E. V.; Barner-Thorsen, C.; Aime, S.; Osella, D.; Gobetto, R.; Milone, L. *Organometallics* **1984**, *3*, 1790.

(30) Mlekuz, M.; Bougeard, P.; Sayer, B. G.; Peng, S.; McGlinchey, M. V.; Mannetti, A.; Saillard, J.-Y.; Naceur, J. B.; Menzen, B.; Jaouen, G. *Organometallics* **1985**, *4*, 1123.